

KG-5
OF
85-25

WATERS' METHOD
SYNTHETIC SEISMOGRAMS
APPLIED TO
SEISMIC REFLECTION MODELING

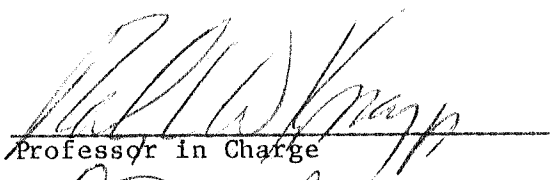
by

Gregory W. Neely

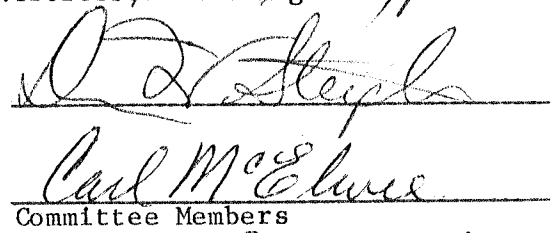
B.A., William Jewell College, 1981

Submitted to the Department of
Physics and the Faculty of the
Graduate School of the University
of Kansas in partial fulfillment
of the requirements for the degree
of Master of Science.

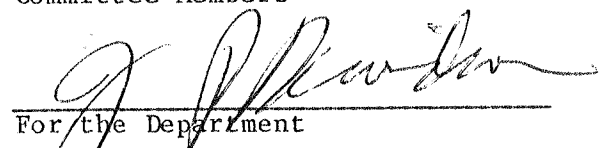
Thesis
1985
N 293
C.2
Science



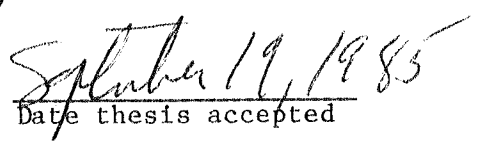
Professor in Charge



Committee Members



For the Department



Date thesis accepted

Kansas Geological Survey
Open-file Report

Disclaimer

The Kansas Geological Survey does not guarantee this document to be free from errors or inaccuracies and disclaims any responsibility or liability for interpretations based on data used in the production of this document or decisions based thereon. This report is intended to make results of research available at the earliest possible date, but is not intended to constitute final or formal publication.

ACKNOWLEDGEMENTS

I want to thank some geophysical professionals who provided invaluable technical assistance for this thesis. Ralph Knapp and Carl McElwee knew the mechanics of preparing synthetic seismic data and shared in the development of theoretical aspects of the program, SYNthesize. George Lam and Dana Adkins-Heljeson caught some pesky bugs in the program. Dao Somanas reprocessed one of the sinkhole lines producing an outstanding product that made modeling easier. John Doveton provided some excellent velocity logs. Rick Miller and Jeff Treadway have been involved with sinkhole data acquisition and processing, and both have made useful suggestions. A special thanks to Rick who was a coconspirator in almost all aspects of working with the real data, from acquisition to interpretation, and who has a gift for asking tough questions at the right time. Don Steeples' geological insights were consistently and frighteningly correct at some times when all I could do was scratch my head and wonder, "What next?"

Other professionals include Young-Jun Chung who spends half of his waking hours in the frequency domain, while helping me to do the same, at least in one dimension. Bill Stahl and Pat Moore were helpful in producing plots. Brett Bennett and Jim Deputy provided rapid solutions to data transfer problems, allowing Esther Price to produce a coherent, nice looking final copy of this thesis. Janice Sorensen provided vital research materials through the Kansas Geological Survey library, and Rex Buchanan's shared literary expertise was appreciated.

Renate Hensiek turned me into a fair draftsman in an unfairly short time, and Pat Acker produced some beautiful photos of these figures.

The number of individuals who freely helped me is indicative of the attitude that is pervasive at the KGS, and explains why I have enjoyed working here so much for the last three years. The moral, physical, and financial support provided by these and other friends at the Survey, and my family, gave me what I needed to get it done.

Thanks everybody.

ABSTRACT

SYNSIZE, a Fortran 77 computer program, was written to generate synthetic seismic responses from well log analyses. The program algorithm solves the one-dimensional wave equation in the frequency domain for plane waves normally incident on flat layers. An inverse fast Fourier transform produces a time domain trace including primaries and multiples.

Linear frequency dependent attenuation and a lithology dependent dissipation factor, Q , are included. This facilitates simulation of pulse broadening with depth and allows variable attenuation of surface multiples.

The program is applied to interpretation of two proposed geologic models for a salt dissolution sinkhole in Ellsworth County, Kansas. Correlation of reflections favors the second model. The generated synthetic traces closely approximate real stacked CDP (common depth point) data.

TABLE OF CONTENTS

	Page
Acknowledgements	i
Abstract	iii
List of Illustrations and Tables	v
Introduction	1
Justification	3
Nature of Q and Attenuation	11
Algorithm Theory	14
Critique of Program SYNSIZE	24
Model Set 1 - Q, Pulse Width, and Phase Shifted Wavelets	30
Model Set 2 - Simulation of Multiples	35
Model Set 3 - A Case Study in Modeling Seismic Reflection Data	42
General Conclusion	59
References	60
Appendices	
1 Fortran 77 code for program, SYNSIZE	64
2 Parameters for Model Set 3, model 1	81
3 Parameters for Model Set 3, model 2	82

LIST OF ILLUSTRATIONS AND TABLES

Figures		Page
1	Classification of multiples	5
2	Nature of seismic waveforms	7
3	Normal incidence CDP approximation	9
Table 1	Synopsis of internal friction parameters	12
4	Upcoming and downgoing waves	18
5	Position for wave amplitude ratios	23
6	Mode conversions	25
Table 2	Multiple amplitude analysis	28
8	Geologic model set 1	32
9	Model Set 1 - Zero phase response	33
10	Model Set 1 - Phase shifted response	34
11	Model Set 2 - Primary events	37
12	Model Set 2 - Surface multiples	38
13	Model Set 2 - Double multiples	39
14A,B	Model Set 2 - Peg-leg multiples	40, 41
15	Location of sinkhole lines	43
16	Relevant geologic units	45
17	Comparison of gamma ray logs	47
18	Q inverse vs. velocity	51
19	Model Set 3 - Model 1	53
20	Model Set 3 - Model 2	54
21	Model Set 3 - Real data from line 1	57

INTRODUCTION

Synthetic seismograms, computer-generated artificial seismic data, are widely accepted within the geophysical community as a tool for modeling the seismic response of sedimentary sequences. For example, from April 1984 to March of 1985, 80 technical articles classified under the heading "Seismic" appeared in print in the Society of Exploration Geophysicists' journal Geophysics. Of these, 36 employed synthetic seismograms in modeling seismic response.

The ubiquitous nature of these models can be explained. The goal of all modeling is to ensure that the seismic section represents the geologic cross section and can be related unambiguously to it. Simply stated, a match must exist. Modeling is instrumental in accomplishing this objective in three ways.

The first is the simulation of multiples. Peg leg, first and higher order multiples, are commonly present on real seismic data and can be easily misinterpreted to represent a lithologic interface. A synthetic seismogram capable of generating multiples can aid in determining whether events on the actual stacked data represent bedding contacts (real geology) or multiples (transmission effects).

Secondly, a match is facilitated by modeling through simulation of pulse width effects of dispersion and the simulation of the sedimentary sequences' collective characteristics as a filter. Studies by Widess (1973,1982) and Kallweit and Wood (1982) have tied the ability of the seismic pulse to detect geologic structure, especially

thin beds, with the pulse width or time length of a seismic pulse. A model displaying changes in pulse width within the rock units, whether source or transmission dependent, enables the modeler to understand the effect exerted by various source bandwidths and lithologies on seismic response. Rocks tend to filter and disperse seismic waves and these effects will ultimately determine how the rocks limit observational tools, particularly in sequences dominated by thin beds.

Finally, the simulation of response on a high speed digital computer allows one to ask "what if?". Many geologically sensible models exist for an observed seismic response. Without simulation, one cannot quantitatively address the question of cause and effect for the geologic sequence and the seismic response. Specifically, questions of how changing lithology, ordering, and thicknesses of rock units affect the seismic record go completely unanswered without some kind of modeling. Modeling is a quantitative link between the geologic units on the cross section and the reality of the seismic reflections. This linking cannot be done with a pencil and paper "thumbnail" calculation, especially with multiple layers.

JUSTIFICATION

Seismic reflection modeling programs may be grouped into either time domain or frequency domain methods. The former group was the first to be developed. The latter hinged upon the development of the fast Fourier transform (FFT).

Four major synthetic seismogram techniques performed in the time domain are those of Peterson et al. (1955), Wuenchel (1960), Robinson and Treitel (1980), and Trorey (1962).

Peterson et al. (1955) derive the reflection coefficient sequence from velocity logs. They neglect multiple reflections and frequency dependence of attenuation, and rely upon a nonlinear logarithmic transformation to arrive at the reflection coefficient log from the velocity log. A wavelet is then placed at each reflection coefficient location, simulating the seismic response.

Further refinement of Peterson's method was achieved by Wuenchel (1960) who was the first to address the problem of producing multiple reflections on synthetic records. Inclusion of multiples becomes a particularly significant feature because in many cases part of the attenuation on seismograms can be attributed to intrabed multiples rather than to the intrinsic properties of rock materials. Schoenberger and Levin (1974) have estimated that attenuation due to intrabed multiples and energy partitioning associated with layering accounted for one-third to one-half of the total frequency dependent attenuation estimated from field seismograms at well locations.

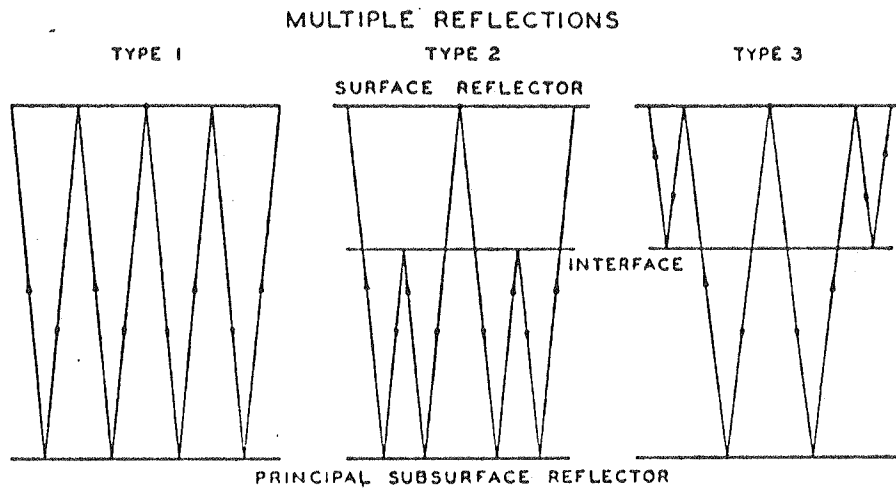


Figure 1A - Classification of multiple reflections, from Ellsworth (1948).

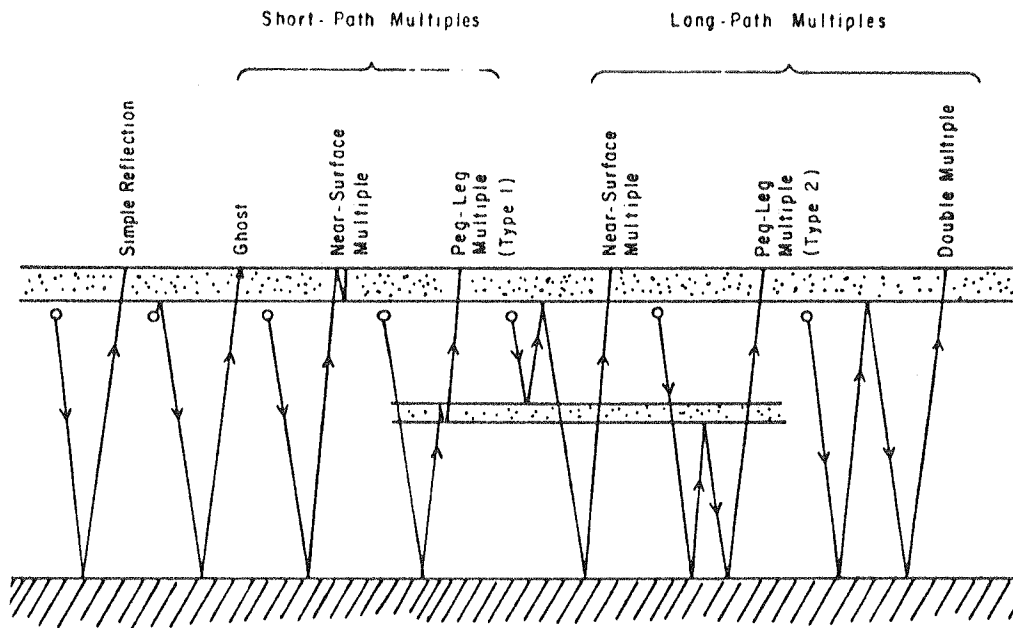


Figure 1B - Classification of multiple reflections, from Sheriff (1984).

account for a broadened seismic pulse with increasing traveltime. Little, if any, agreement exists about even the most fundamental processes causing attenuation. Kjartansson (1979) reviewed papers on attenuation by 25 authors and concluded that a fundamental feature associated with the propagation of stress waves in all real materials is the absorption of energy and the resulting change in the shape of transient waveforms.

Trorey's (1962) method is the most sophisticated of the time domain methods mentioned, employing frequency dependent absorption in the calculated response. Network theory is employed to minimize execution time, so the method is practical for iterative modeling. This method produces records with all primaries and peg-leg multiples or all primaries and multiples. Figure 2 shows theoretical waveforms from Ricker (1953) supporting frequency dependence of the attenuation. The resulting waveform shape is basic to seismic resolution since the precise delineation of reflecting beds cannot be properly addressed unless the form of the seismic disturbance at depth is modeled. Inclusion of frequency dependent attenuation is the principal advantage of Trorey's method (1962) over that of Robinson and Treitel (1980).

Frequency domain approaches are patterned after the pioneering work of Thompson (1950) describing the theory of reflections of a plane wave from a layered elastic system. All such approaches perform the main body of computation in the frequency domain for each constituent plane wave over a designated bandpass. An inverse FFT is

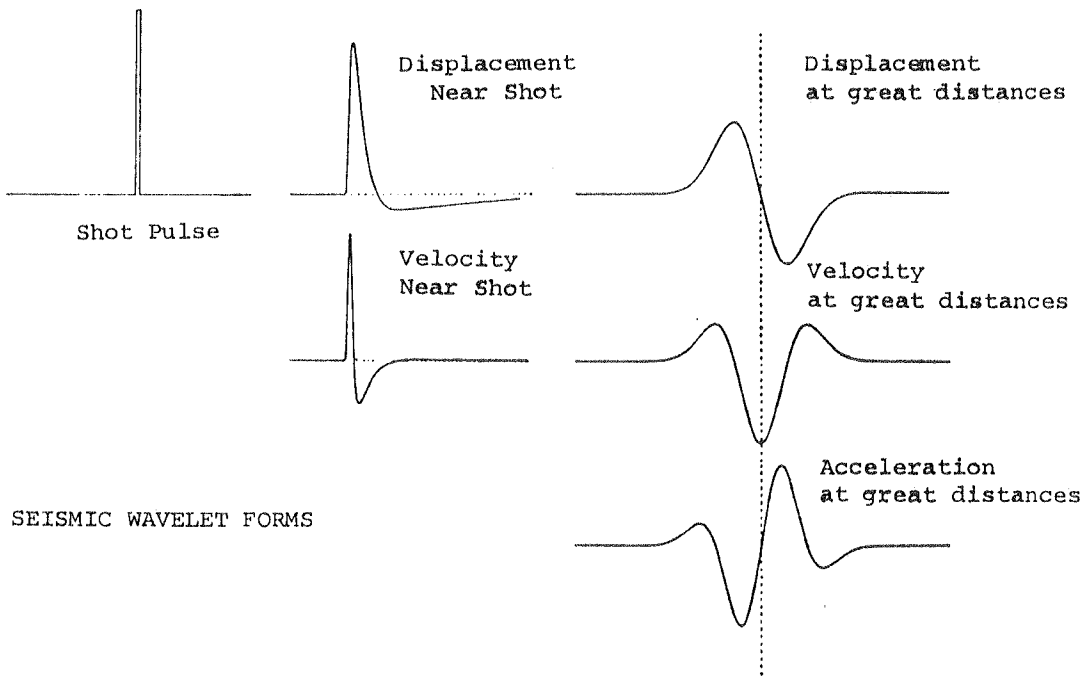


Figure 2 - Ricker (1953)
Nature of Seismic Waveforms

performed to bring the response back into the time domain. This is the essence of Waters' algorithm and is a basic description of SYNSIZE, (Appendix 1), the method and program used in this thesis.

Thus far, all of the methods mentioned assume wave propagation in the z direction only, i.e. perpendicular to flat lying layers. This is not a tremendous handicap because normal incidence seismic response algorithms yield a trace that is an excellent approximation to the typically displayed stacked CDP (common depth point) response. Figure 3 shows that the application of normal moveout to a CDP gather forces all of the traces from a common reflecting point to approximate a normal incidence trace. The shortcomings of this approximation are discussed in the critique section of this thesis.

Kennett (1978) discusses a method capable of generating the response of multiple layers for nonnormal incidence. The output model is in the form of a field file rather than an approximation to stacked data. His method is probably the most sophisticated for many layered systems to appear in print to date, with the desirable attributes of optional multiples, frequency dependent attenuation, and mode conversions. The drawback is that the layers must be flat, as was the case for Waters' (1981) and previous methods.

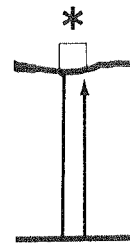
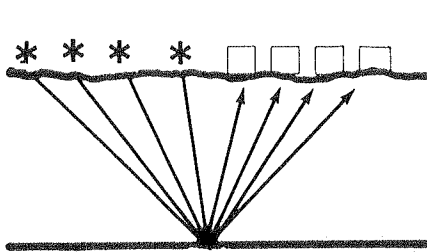
The critical nature of sophisticated synthetic seismogram programs is pointed out by Waters (1981). He lists some specifications of state of the art programs, some of which are proprietary or available for purchase or lease. Common to all of these programs is the inclusion of curvilinear boundaries to simulate real geologic struc-

GEOMETRY

Shooting
CDP

Shooting
Normal Incidence

* = Shot points
□ = Receiver locations



FIELD FILES



CDP

Normal Incidence Product

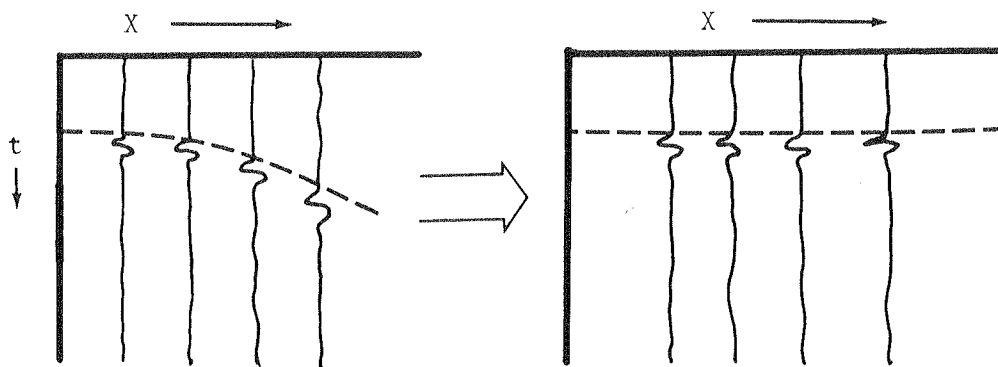


Figure 3 - Application of Normal Moveout to a CDP Field File. Product looks like normal incidence data for a flat reflector.

tures. This inclusion, however, results in the abandonment of mode conversion and frequency dependent attenuation modeling capability because the execution time with these options becomes prohibitive for arbitrary geologic structures.

NATURE OF Q AND ATTENUATION

Qualitatively, the symbol "Q" has been used to denote the quality of a rock for seismic wave propagation. Parenthetically, "Q" was used long before it was applied to rocks in describing the quality in electronic filtering. A homogeneous solid would be perfectly elastic with a Q of infinity; the strain at any point being directly proportional to the instantaneous stress. A wave once generated in such a medium would have finite energy and would propagate indefinitely. Experiments have demonstrated that this perfect medium is not a realistic approximation of earth materials. Elastic vibrations subside; undergo damping, even when the material is isolated from its surroundings (Bradley and Fort, 1966).

The means of best expressing the internal friction parameters, i.e. those parameters relating to the nonelastic damping mechanisms in earth materials converting strain energy into heat, is open to question. Table 1 lists some quantities that are in common use and the relationship of the listed parameters to the expression for damped plane waves in an infinite medium.

The nature of the energy losses per cycle may be classified as linear or nonlinear, constant Q (CQ) or nonconstant Q (NCQ) with the possibility of band limited near constant Q (Kjartansson, 1979). The fact that strains less than .001 demonstrate no amplitude dependence of the propagation velocity or Q substantiates the view that earth materials response is dominated by linearity (Brennan and Stacy,

The symbols for and brief definitions of some of the other internal friction parameters are:

$1/Q$ = specific dissipation constant—the tangent of the phase angle by which the strain lags behind the applied stress in the case of sinusoidal excitation. It is related to the rate at which the mechanical energy of vibration is converted irreversibly into thermal energy and thus does not depend on the detailed mechanism by which the energy is dissipated

δ = logarithmic decrement—the natural logarithm of the ratio of the amplitudes of two successive maxima or minima in an exponentially decaying free vibration

a = damping amplitude coefficient in the expression for a free vibration:

$$e^{-at} \sin 2\pi ft$$

α = attenuation coefficient in the expression for plane harmonic waves in an

infinite medium: $e^{-\alpha x} \sin 2\pi f \left(t - \frac{x}{c} \right)$ where c = wave velocity

D = damping ratio, defined by analogy with simple second-order systems

$\Delta f/f$ = relative bandwidth of resonance curve between the half-power or 0.707 amplitude points for a solid undergoing forced vibrations—is a measure of the sharpness of the response curve

$\Delta E/E$ = fraction of strain energy lost per stress cycle.

By using the analogy of a simple linear second-order vibrating system b , the specific damping capacity, may be related to the other parameters as indicated:

$$b = 2\pi/Q = 2\delta = 2 \frac{a}{f} = 2c \frac{\alpha}{f} = 4\pi D = 2\pi \frac{\Delta f}{f} = \frac{\Delta E}{E}$$

Table 1 - Synopsis of internal friction parameters
(Bradley and Fort, 1966).

1977). This means that the strain resulting from the superposition of two stress functions is the same as the sum of the strains resulting from application of each stress function separately.

In theory, Bland (1960) and Strick (1967) have shown that a particular form of the stress-strain relationship leads to a Q that is independent of frequency, synonymous with a CQ model. This model satisfies causality, since the derived creep functions and relaxation functions (plotting strain versus time and stress versus time respectively) are zero for negative values of time.

Experimentally, results obtained in the Pierre Shale by McDonal et al. (1958) and Ricker (1953) are consistent with a linear CQ model. McDonal's results indicated that "individual Fourier components of the waveforms decay exponentially and that the decay was proportional to the frequency". Even though Ricker fitted his pulse width versus travel time data with a NCQ function, Kjartansson (1979) has reanalysed Ricker's field data producing a comparable fit to a CQ model.

Johnson and Toksoz (1981) give an excellent overview of the current state of affairs in Q models:

A reasonable conclusion from existing data is that the amplitude of the seismic response model should be attenuated exponentially by a coefficient whose frequency dependence is linear.

ALGORITHM THEORY - Waters' Synthetic Seismogram

This section gives a detailed description of the frequency domain approach used in the program SYNSIZE (Appendix 1) to generate a CQ model synthetic seismogram for normal incidence. The program uses an iterative solution to obtain ratios of up to downgoing cumulative wave component amplitudes for interfaces bounding layers with no dip by solving the one-dimensional wave equation in the frequency domain. Most of the computations are based directly on Waters' (1981) algorithm.

An inverse fast Fourier transform (FFT) operates on the frequency domain response calculated for each frequency to obtain a final time domain output.

The algorithm assumes a complex phase velocity:

$$c = V + i\nu \quad (1)$$

where: V = the scalar interval velocity for a given layer, and
 ν = the imaginary attenuation component.

A complex representation for the velocity allows convenient handling of frequency dependent attenuation.

An often used form for the wave equation in one dimension:

$$\frac{\partial^2 \zeta}{\partial t^2} = c^2 \frac{\partial^2 \zeta}{\partial x^2} \quad (2)$$

has a solution of the form:

$$\zeta = \zeta_0 \exp \left\{ i\omega \left[t - \frac{x}{c} \right] \right\} \quad (3)$$

where:

ζ = the displacement of the wave,

ζ_0 = the initial displacement,

ω = the angular frequency of the wave,

x = the axis along which the wave is moving, and

t = time.

The complex velocity substitution (1) into (3) yields:

$$\zeta = \zeta_0 \exp \left\{ i\omega \left(t - \left[\frac{x(V-i\upsilon)}{V^2 + \upsilon^2} \right] \right) \right\}.$$

This equation can be simplified by assuming that $\upsilon^2 \ll V^2$, i.e. that the square of the scalar velocity is much larger than the square of the imaginary attenuation component. This assumption seems intuitively correct, since attenuation coefficients are usually much smaller than one, while velocities are measured in thousands of feet per second. The above assumption results in a familiar exponentially attenuating form for the wave equation. Now:

$$\zeta = \zeta_0 \exp \left\{ i\omega \left(t - \frac{x}{V} + \frac{x i \upsilon}{V^2} \right) \right\}.$$

Regrouping as the product of two exponential terms:

$$\zeta = \zeta_0 \exp \left\{ i\omega \left(t - \frac{x}{V} \right) \right\} \exp \left\{ -\omega \frac{UX}{V^2} \right\}. \quad (4)$$

Note that (4) is (3), multiplied by an exponential coefficient.

Equation (4) may be rewritten:

$$\zeta = \zeta_0 \exp \left\{ i\omega \left(t - \frac{x}{V} \right) \right\} \exp (-\alpha x). \quad (5)$$

Inspection of (4) and (5) yield the attenuation coefficient:

$$\alpha = \frac{\omega U}{V^2}.$$

This result may be related to another empirically derived formula:

$$\alpha = \frac{\pi f}{QV} \quad (6)$$

where:

Q = the quality factor, independent of frequency (CQ model),

f = the frequency of the attenuated wave,

V = the scalar velocity.

Equation (6) appears in Dobrin (1976) who cited first power frequency dependence in samples of shale, sandstone, limestone and

"caprock". Kjartansson (1979) has documented a multitude of mechanisms resulting in this form of attenuation.

Setting:

$$\frac{wU}{v^2} = \frac{\pi f}{QV} \quad (7)$$
$$\frac{2U}{V} = \frac{1}{Q} .$$

The assumption $U^2 \ll V^2$ now seems reasonable. The inverse of Q is always much smaller than one for lithified media, (Bradley and Fort, 1966) hence (7) is a small number, supporting $U^2 \ll V^2$.

Given the exponential form for the wave equation (5), wave interaction with multiple interfaces can be simulated. Figure 4 (Waters, 1981) shows the wave state for two consecutive layers.

The changes in sign occurring within each mathematical representation of an upcoming or downgoing wave as shown in Figure 4 can be explained, since equation (5) represents a wave traveling in the positive x direction. In each layer, there are upcoming waves of amplitude A^- and downgoing waves of amplitude A^+ . Since the waves attenuate as they travel through the layer, the amplitudes A_m^- and A_m^+ are measured at points one and two respectively. The same convention applies to A_{m+1}^- and A_{m+1}^+ at points three and four, also labeled in Figure 4.

Often, the derivation of a particular solution to a partial differential equation, e.g. equation (2), depends upon the specifi-

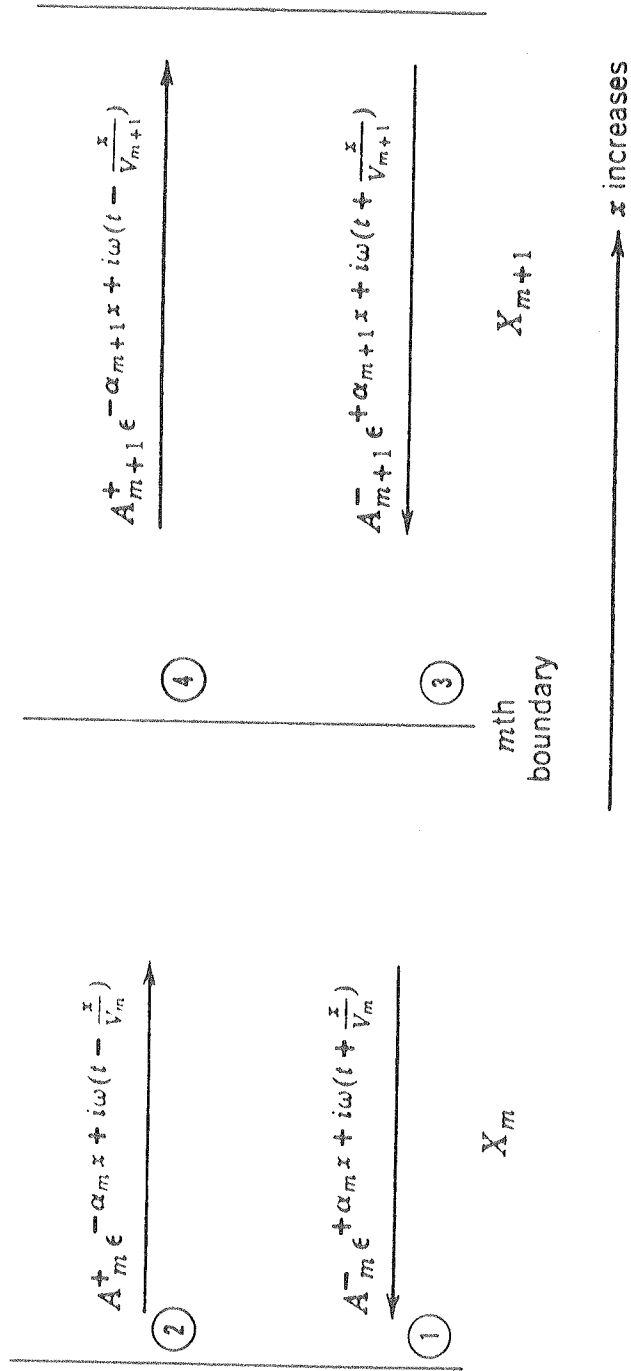


Figure 4 - Up and downgoing waves in two consecutive layers (Waters, 1981).

cation of one or more boundary conditions. These boundary conditions are a mathematical expression of a physically realistic set of conditions that are applicable to the model used in approximating reality.

Consider a seismic wave propagating across a geological contact between flat-lying strata. A certain amount of energy is transmitted across this interface, and a certain amount is reflected back towards the surface. At no time, however, does a separation take place along the contact because of the minute energy of the wave upon the interface. Mathematically, this concept of continuity of displacement can be expressed at a boundary or contact, using the previously defined wave formulae, as:

$$\begin{aligned}
 & A_m^+ \exp \left\{ -\alpha_m x_m - (i\omega x_m / V_m) \right\} \\
 & + A_m^- \exp \left\{ -\alpha_m x_m + (i\omega x_m / V_m) \right\} \\
 & = A_{m+1}^+ + A_{m+1}^- .
 \end{aligned} \tag{8}$$

It is also reasonable to require stress continuity across the boundary (Garland, 1979):

$$c_m^2 \rho_m \left(\frac{\partial \zeta_m}{\partial x} \right)_{x=x_m} = c_{m+1}^2 \rho_{m+1} \left(\frac{\partial \zeta_{m+1}}{\partial x} \right)_{x=0} . \tag{9}$$

Because ζ_m is the particle displacement due to the combination of upcoming and downgoing waves, (9) may be rewritten as:

$$c_m^2 \rho_m \left(\frac{\partial \zeta_m^+}{\partial x} + \frac{\partial \zeta_m^-}{\partial x} \right)_{x=x_m} = c_{m+1}^2 \rho_{m+1} \left(\frac{\partial \zeta_{m+1}^+}{\partial x} + \frac{\partial \zeta_{m+1}^-}{\partial x} \right)_{x=0}. \quad (10)$$

Using the formulae in Figure 4 to define ζ_m^+ , ζ_m^- , ζ_{m+1}^+ and ζ_{m+1}^- the partial derivatives of equation (10) may be calculated and substituted into (9) (Waters, 1981) and evaluated at $t=0$:

$$\begin{aligned} & c_m^2 \rho_m \left\{ A_m^+ \left(-\alpha_m - \frac{i\omega}{V_m} \right) \exp \left\{ -\alpha_m x_m - (i\omega x_m / V_m) \right\} \right. \\ & \quad \left. + A_m^- \left(\alpha_m + \frac{i\omega}{V_m} \right) \exp \left\{ \alpha_m x_m + (i\omega x_m / V_m) \right\} \right\} \\ & = c_{m+1}^2 \rho_{m+1} \left[A_{m+1}^+ \left(-\alpha_{m+1} - \frac{i\omega}{V_{m+1}} \right) + A_{m+1}^- \left(\alpha_{m+1} + \frac{i\omega}{V_{m+1}} \right) \right]. \end{aligned} \quad (11)$$

For brevity, define:

$$q = \exp \left\{ -\alpha_m x_m - (i\omega x_m / V_m) \right\}.$$

The ratio of complex acoustic impedances is:

$$K_m = \frac{(V_{m+1} + i\upsilon_{m+1}) \rho_{m+1}}{(V_m + i\upsilon_m) \rho_m}. \quad (12)$$

An alternate form for (12) is:

$$K_m = \frac{\alpha_{m+1} + (i\omega/V_{m+1}) c_{m+1}^2 \rho_{m+1}}{\alpha_m + (i\omega/V_m) c_m^2 \rho_m}. \quad (13)$$

Equation (13) can be proven approximately equivalent to (12) by substituting into (12) and neglecting higher order terms in v . Using (13), equations (9) and (11) reduce respectively to:

$$A_m^+ q + A_m^- / q = A_{m+1}^+ + A_{m+1}^- \quad (14)$$

and:

$$-A_m^+ q + A_m^- / q = K_m (-A_{m+1}^+ + A_{m+1}^-). \quad (15)$$

Representing the ratio of cumulative up to downgoing wave amplitudes measured at the top of the m th layer is easy:

$$R_m = \frac{A_m^-}{A_m^+} \quad R_{m+1} = \frac{A_{m+1}^-}{A_{m+1}^+}. \quad (16)$$

Equation (14) may be divided by (15) to obtain:

$$R_m = q^2 \left(\frac{R_{m+1} + r_m}{1 + R_{m+1} r_m} \right) \quad (17)$$

where:

$$r_m = \frac{1 - K_m}{1 + K_m}. \quad (18)$$

Equation (17) is the general iteration formula used by SYNSIZE to obtain the ratio of up to downgoing cumulative wave amplitudes as a function of a single frequency ω . The calculations must be repeated over each frequency within the designated bandwidth of the response. Note that the formula starts at the bottom of the sequence and iterates upward, until R_0 is obtained.

The problem of initializing the iterative procedure now remains. This is performed by the program within a separate subroutine START. The idea is that no reflection comes from below the mth boundary; the last reflecting interface of the model. This means:

$$R_{m+1} = \frac{A_{m+1}^-}{A_{m+1}^+} = 0 \quad (19)$$

and equation (17) simplifies to:

$$R_m = q^2 r_m \quad (20)$$

for the top of the layer above the mth boundary, as shown in Figure 5.

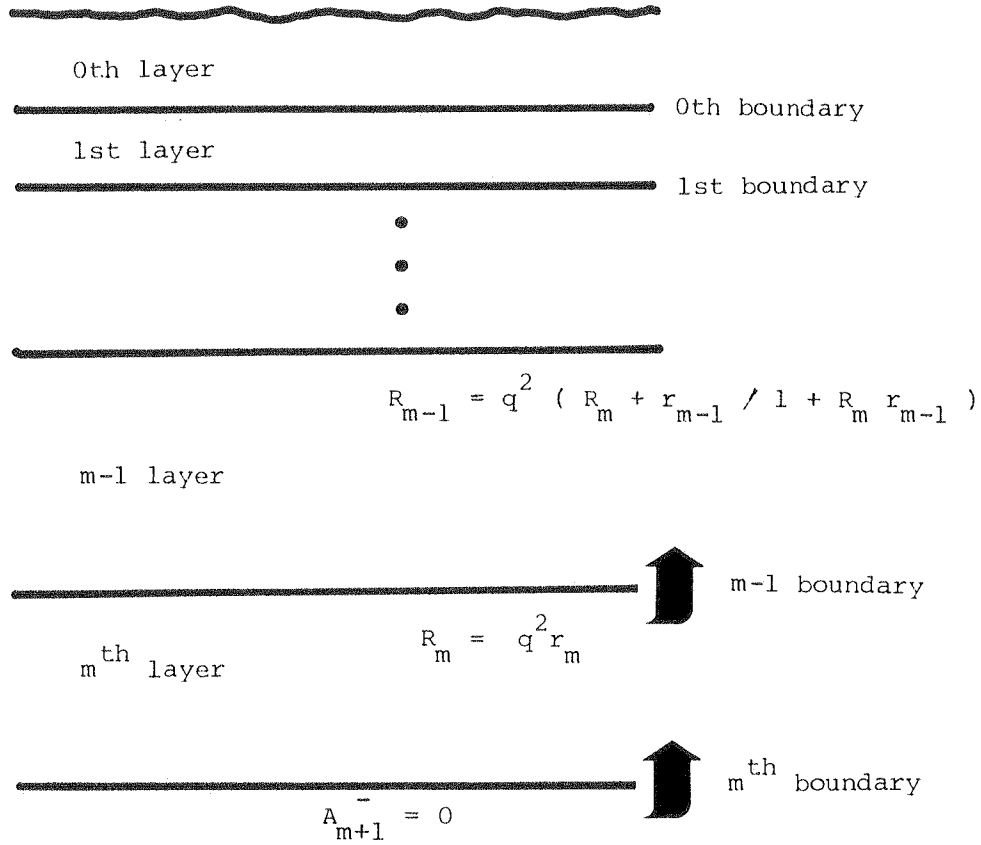


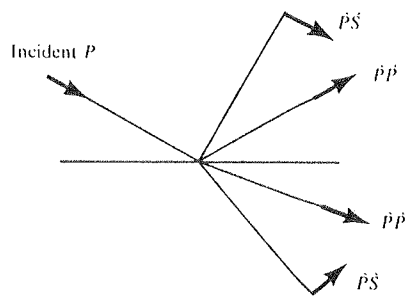
Figure 5 - Position for Cumulative Ratios of Up to Downgoing Wave Amplitudes Calculated in Equations (17), (19), and (20).

CRITIQUE OF PROGRAM SYNSIZE

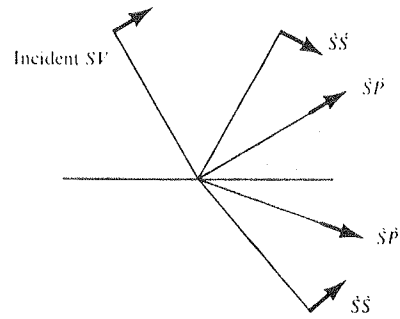
Any method of generating synthetic seismograms has some weaknesses relative to other methods. The algorithm used by SYNSIZE is no exception.

One weakness is the inability of the program to examine the effect on stacked data of nonzero source receiver offsets. The behavior of seismic waves at nonzero offset has been extensively studied. Zero offset modeling fails to simulate mode converted waves, i.e. incident P waves changing into an S waves or vice versa upon interaction with an interface. Aki and Richards (1980) show that nonzero offset considerations quickly deteriorate into a very complicated situation. Figure 6 shows that for a single flat interface, the partitioning of energy is no longer governed by a single reflection coefficient, as in the normal incidence case, but is controlled by "sixteen possible reflection/transmission coefficients".

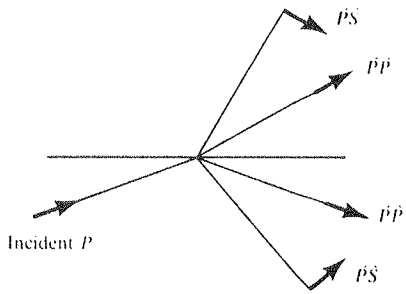
The ability of a program to simulate mode conversions is useful in studying the dependence of seismic body wave amplitudes upon rock parameters. Such amplitude changes are not significant until a large source receiver offset relative to the target depth is used (Morrison, 1984). Reflection and transmission of plane compressional waves for flat interfaces has been studied by Tooley et al. (1965). While the behavior is very complicated, these workers have shown that in general mode conversions do not account for more than twenty percent of the total incident wave energy until angles of incidence of at least



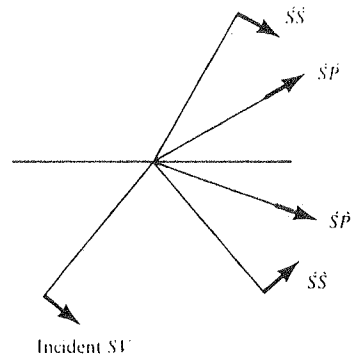
(a)



(b)

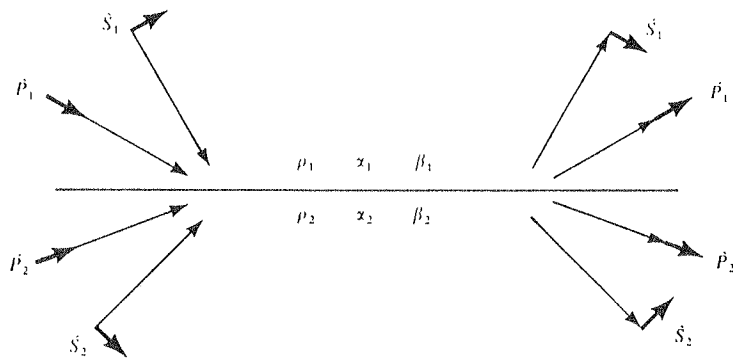


(c)



(d)

Notation for the sixteen possible reflection/transmission coefficients arising for problems of *P-SV* waves at the welded interface between two different solid half-spaces.



The complete system of incident and scattered plane *P-SV* waves, in terms of which the scattering matrix can quickly be found. Short arrows show the direction of particle motion; long arrows show the direction of propagation.

Figure 6 - Mode conversion, from Aki and Richards (1981).

thirty degrees are reached. Typical offsets in surveys performed by the KGS are well below that required to obtain this high of an angle of incidence, so inclusion of mode conversions in a modeling program would have little if any utility in modeling the existing MinisOSIE database. Also, recording of the converted waves at the surface requires a level of sophistication in S wave recording that is not yet widespread in KGS data processing and acquisition. The vast majority of existing data is recorded with vertical geophones. A very small percentage of the recorded vertical signal results from energy that has undergone mode conversion.

There are two more significant shortcomings for the program. The first is that the surface reflection coefficient is not variable for the top of the uppermost bounded layer. In the program the magnitude of this reflection coefficient is always unity. In nature, the marine wave transmission case for a smooth sea approximates this situation. Here, the air water interface has a reflection coefficient whose magnitude is unity because of the high acoustic impedance contrast between water and air and the flatness of the surface compared to the wavelength of the data. Other geological surfaces do not exhibit this behavior partially because the change in acoustic impedance is not as drastic and because other real geological interfaces are often not flat.

Experimental measurements of the reflection coefficient for this interface are rare. Data recorded by Van Melle and Weatherburn (1953)

showed reflection coefficients as high as two-thirds for the base of the Pleistocene Beaumont clay surface in Harris County, Texas.

The program compensates for the lack of adjustment in the reflection coefficient for the uppermost interface. This is in effect modeling one of the causes for a less than perfect surface reflection coefficient. A finite value for Q in the uppermost bounded layer is analogous to an infinite Q with a surface reflection coefficient less than one. A study of the influence of Q in the uppermost bounded layer shown in Figure 7 is summarized in Table 2. Four runs were made on a single bounded layer model with Q being the only varied parameter in each run.

The reflection coefficient for the base of the bounded layer is $-.2605$, as predicted from the model densities and velocities. The normalized maximum reflection amplitude for the first order multiple pulse in Run 1 is $-.2605$, one being the maximum for the primary reflection pulse. Q was infinity for the bounded layer in run 1. This is synonymous with zero attenuation.

Run 2 showed a maximum for the first order multiple pulse of about two-thirds that for the first order multiple of run 1. This is due to the Q value of 500 (still very high, geologically speaking) for the bounded layer in run 2. Since the reflection coefficient for the base of the bounded layer has not changed from run 1 to run 2, the effect of introducing a finite Q in the layer on maximum multiple amplitude is the same as that obtained by changing the reflection coefficient of the uppermost surface to a value less than one. Thus

FIXED PARAMETERS:

air

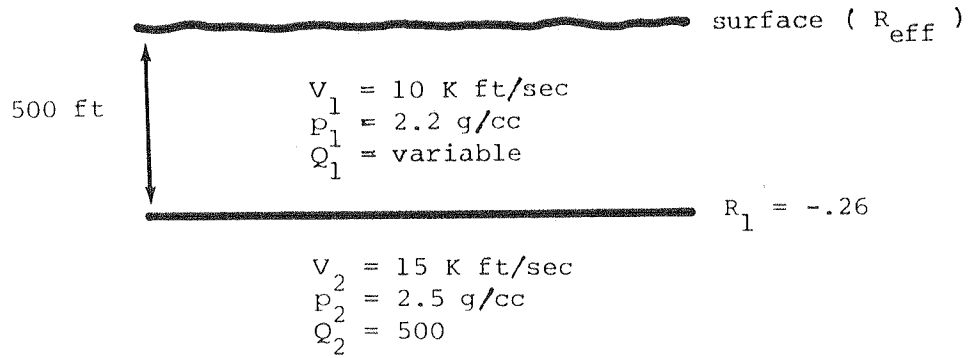


Figure 7 - Bounded layer used in multiple amplitude analysis.

R_n = reflection coefficient for N^{th} layer

R_{eff} = "effective" surface reflection coefficient

Run	Q_1	$ R_{eff} $ first order multiple
1	infinite	1
2	500	.69
3	100	.50
4	20	.49

Table 2 - Influence of Variable Q
on Multiple Amplitudes

the introduction of Q is said to introduce an effective reflection coefficient for the uppermost surface with magnitude less than unity. Runs 3 and 4 demonstrate the lowering Q lowers the effective reflection coefficient.

The final significant area for improvement remaining in the modeling program is the ability to zero out events according to their travel paths, i.e. to obtain a response with primaries only, primaries and first order multiples, primaries and peg-leg multiples, etc. As written, the only option is the response with primaries and all multiples. The geophone cannot make event discriminations in the field. Nevertheless, it would be an advantage to automatically categorize events on a record without doing travel time calculations by hand. A step in this direction can be made by eliminating all surface multiples through a deconvolution described in detail in Claerbout and Riley (1976).

MODEL SET 1 - Q, Pulse width, and phase shifted wavelets

Model Set 1 consists of three different depth models for a single bounded layer whose parameters (Q, velocity and density) are those of the Pierre Shale (Ricker, 1953). This model is shown in Figure 8. The parameters for the lower half space are typical of those encountered for a limestone. The data in all three runs are filtered over a bandpass typically used in MiniSOSIE CDP data processing at the KGS.

Observe first the increase in reflection pulse width with increasing depth or travel time, comparing runs one, two, and three in Figure 9. This is predictable from the CQ model upon which the algorithm is based. More travel time through the shale allows more pulse broadening. This is also an attenuation effect; the energy is concentrated in the central portion of the pulse due to less attenuation at shallow depth.

The response after adding a 90 degree phase shift is shown in Figure 10. The same geologic parameters apply. The spreading of pulse energy due to attenuation with depth is now more visible.

Conclusions - Model Set 1

The reflection pulses produced by SYNSIZE for a set of single bounded layers demonstrate increasing pulse width with increasing travelttime. This effect can be attributed to the inclusion of frequency dependent attenuation in the modeling algorithm. The response is consistent with models in which the attenuation coefficient is

proportional to the first power of the frequency, i.e. a linear attenuation model.

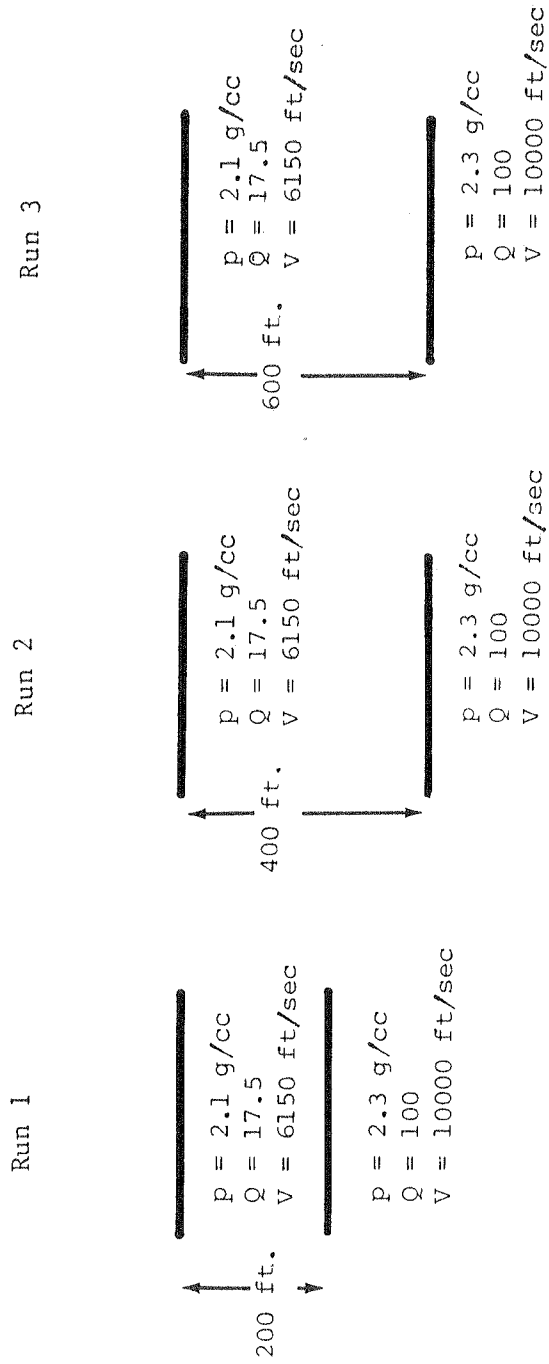
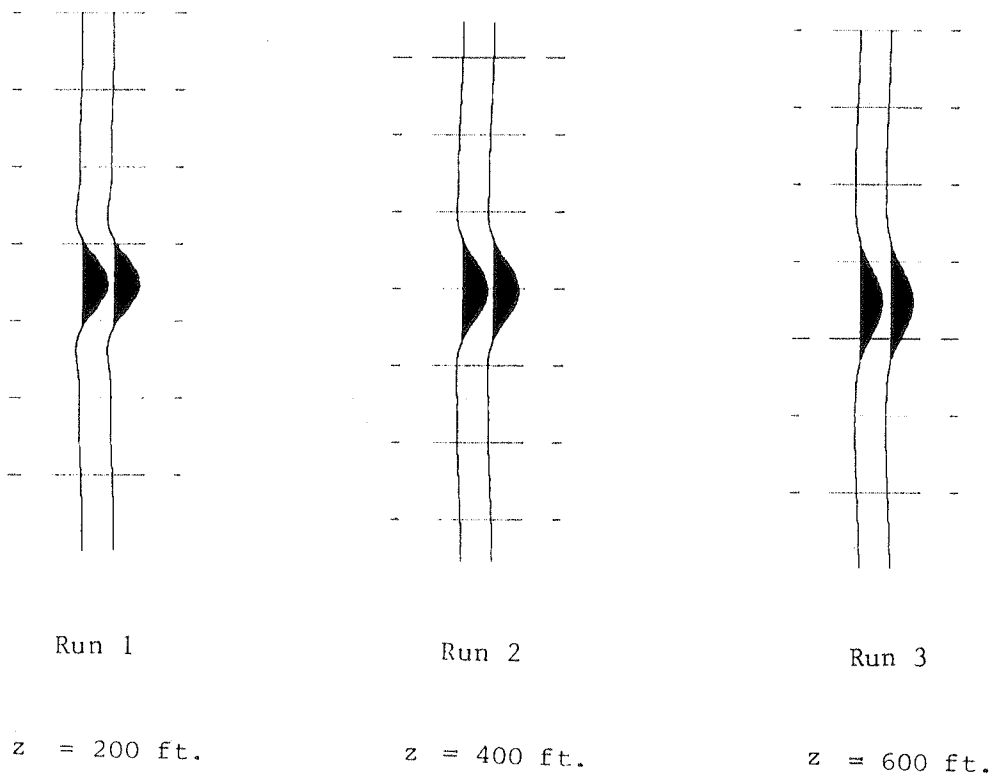


Figure 8 - Geologic Model Set I

ZERO PHASE RESPONSE

Model Set 1

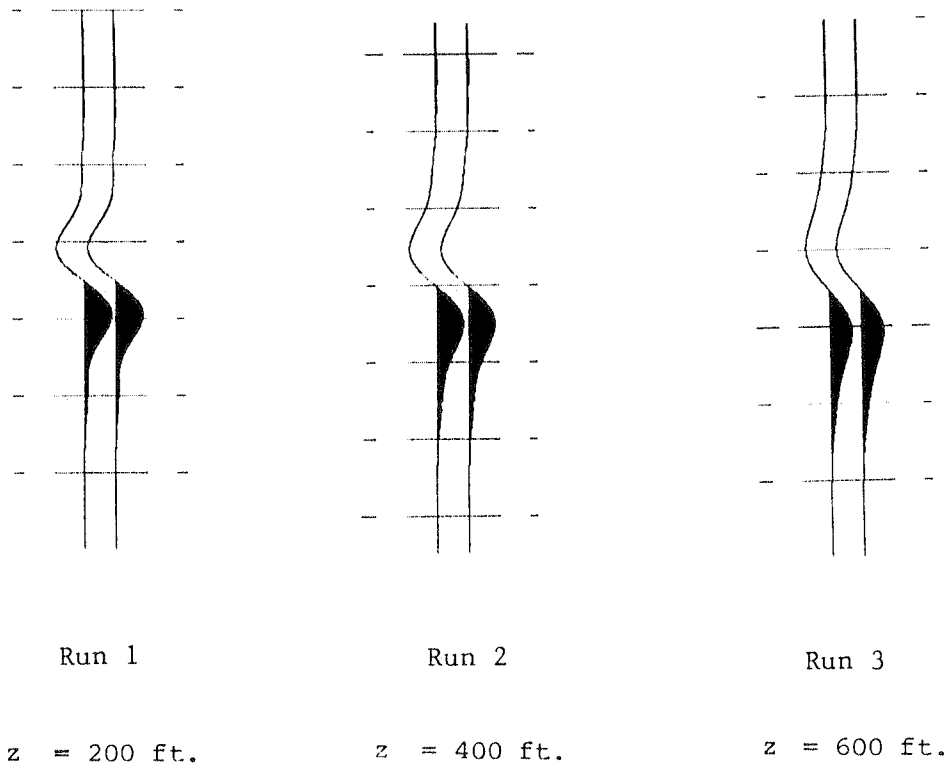


$z = \text{length of travel path}$

Figure 9 - Increasing travel path length results in broadening of the seismic event. (timing lines spaced at 10 msec)

PHASE SHIFTED RESPONSE

Model Set 1



$z =$ length of travel path

Figure 10 - Increasing travel path length results in broadening of the seismic event.
(timing lines spaced at 10 msec)

MODEL SET 2 - Simulation of multiples

Figures 11 through 14B demonstrate SYNSIZE's ability to generate all transmission effects anticipated from a plane wave with normal incidence on flat layers.

Figures 11 and 12 identify the primary and near surface multiple reflection events respectively for a geologic model with three bounded layers. Figure 13 identifies double multiples, while Figures 14A and 14B identify the peg-leg multiples. The parameters chosen simulate a low velocity sand imbedded in a shale layer; a frequently encountered geological situation.

A brief explanation of the notation used to identify events in Figures 11 through 14B is appropriate. An upper case P with a number i denotes a reflection from the base of the i th layer. A lower case p followed by a number i is used to identify an event reflected from the top of layer i . Thus, $P_3p_1P_2$ would describe an event reflected from the base of the third layer, top of the first layer, and base of the second layer, in order.

Generation of troublesome multiples is common in this situation. The high amplitude of some of the multiple events relative to the primaries can be attributed to the application of automatic gain control (AGC). Events of this amplitude on a seismic record with AGC applied might easily be confused with a real geologic interface, such as a bedding contact. Parenthetically, deconvolution is particularly effective in reducing surface multiples, but peg-leg multiples are not

as easily removed with deconvolution techniques. A modeling program that can generate peg-leg multiples is particularly useful in interpreting a deconvolved section.

Conclusion - Model Set 2

Each primary and multiple event labeled in this model set possesses a polarity and an arrival time corresponding to those predicted from the chosen three bounded layer model. The response of the model did not include attenuation. This facilitated clear identification of deeper primaries and multiples. Since the ability of the program to simulate transmission effects is proven, SYNSIZE may now be applied to more complicated geologic models.

Geologic Model Set 2

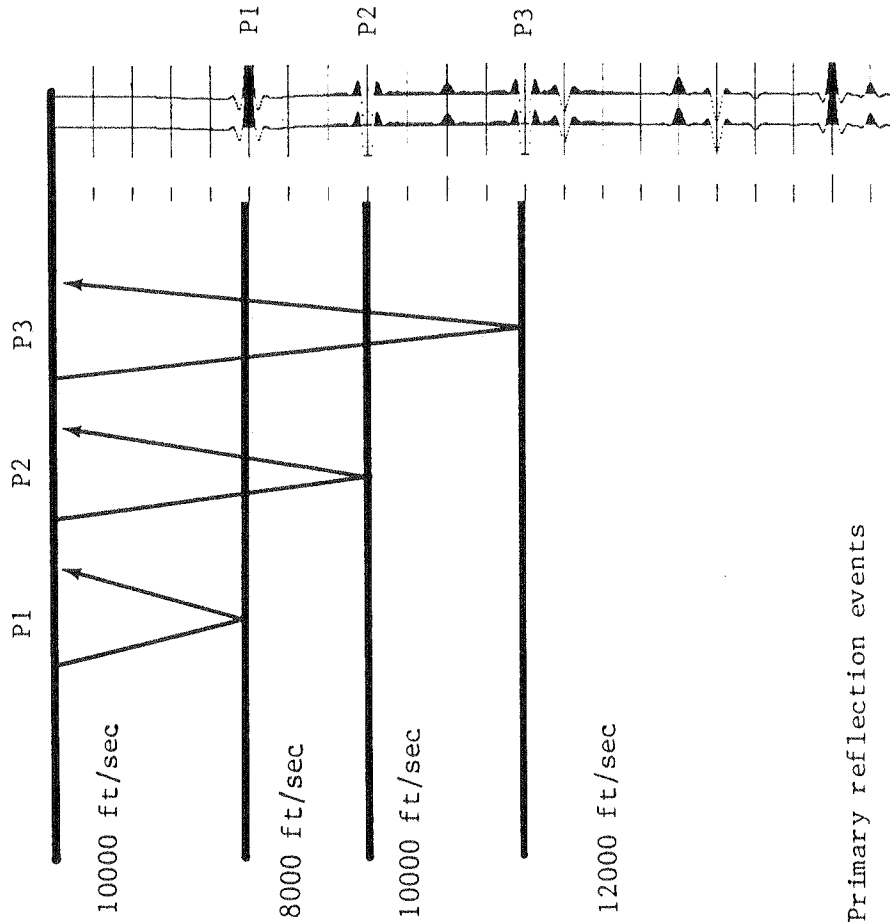


Figure 11 - Primary reflection events
Zero phase response with no attenuation
(timing lines spaced at 10 msec)

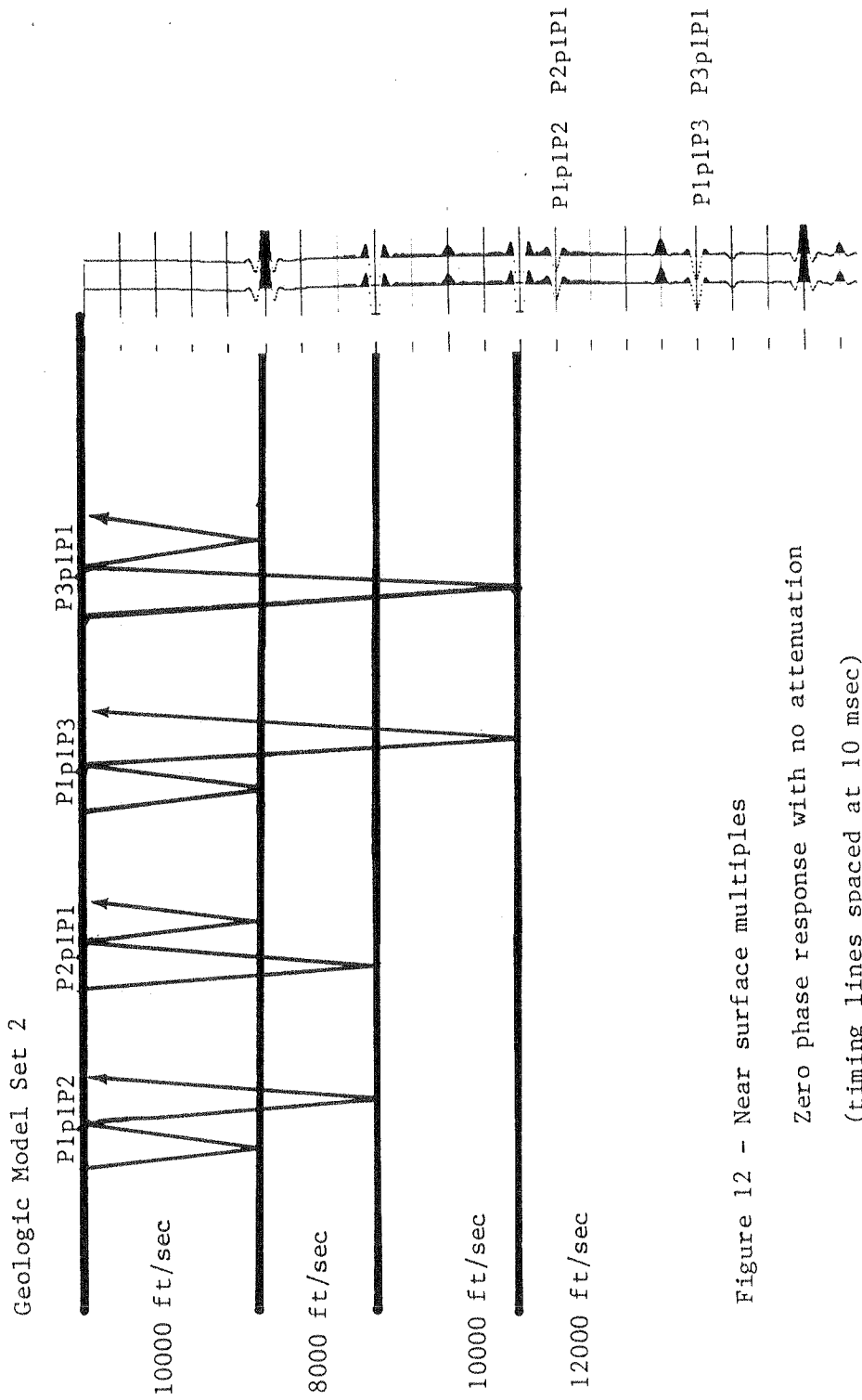


Figure 12 - Near surface multiples

Zero phase response with no attenuation
 (timing lines spaced at 10 msec)

Geologic Model Set 2

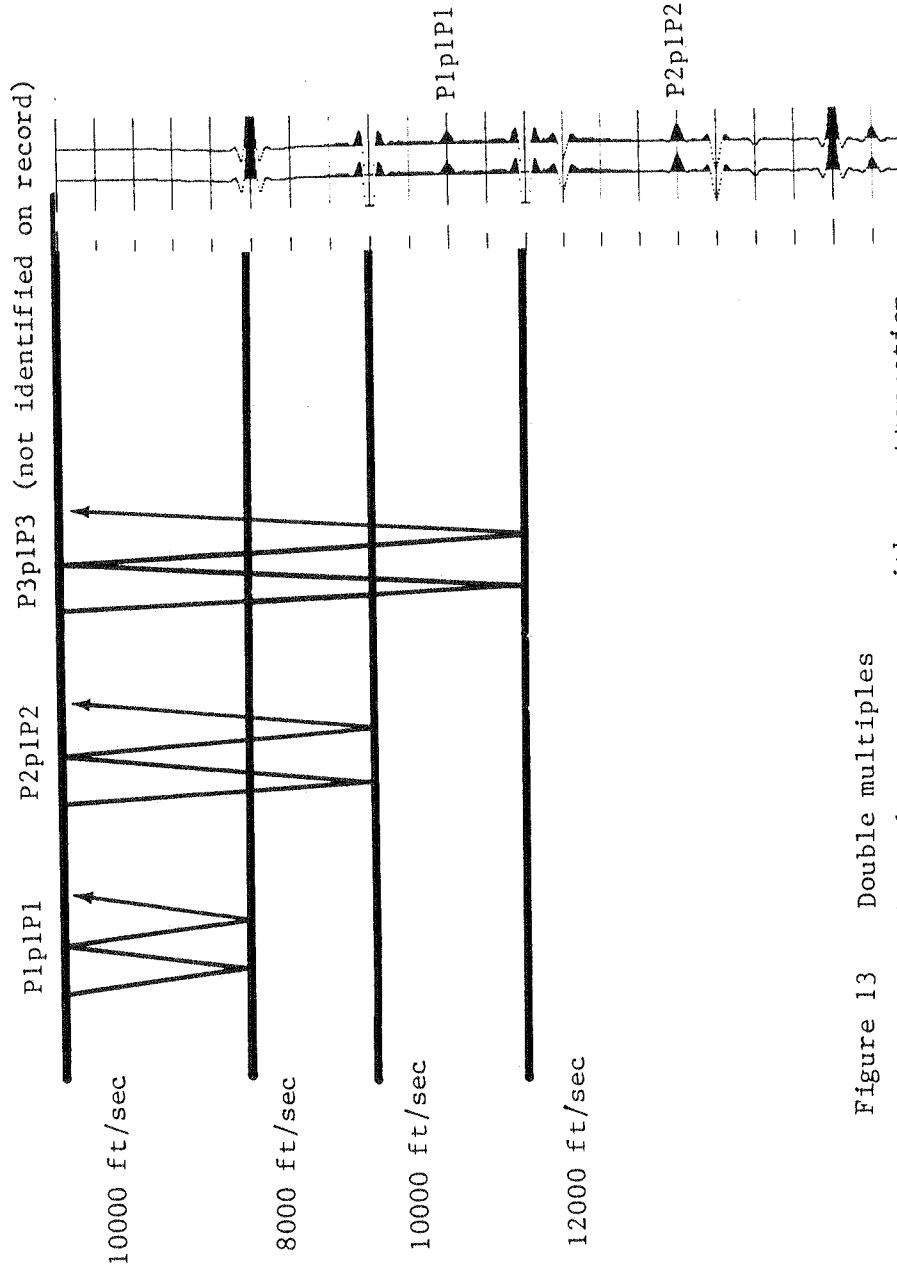


Figure 13 Double multiples
Zero phase response with no attenuation
(timing lines spaced at 10 msec)

Geologic Model Set 2

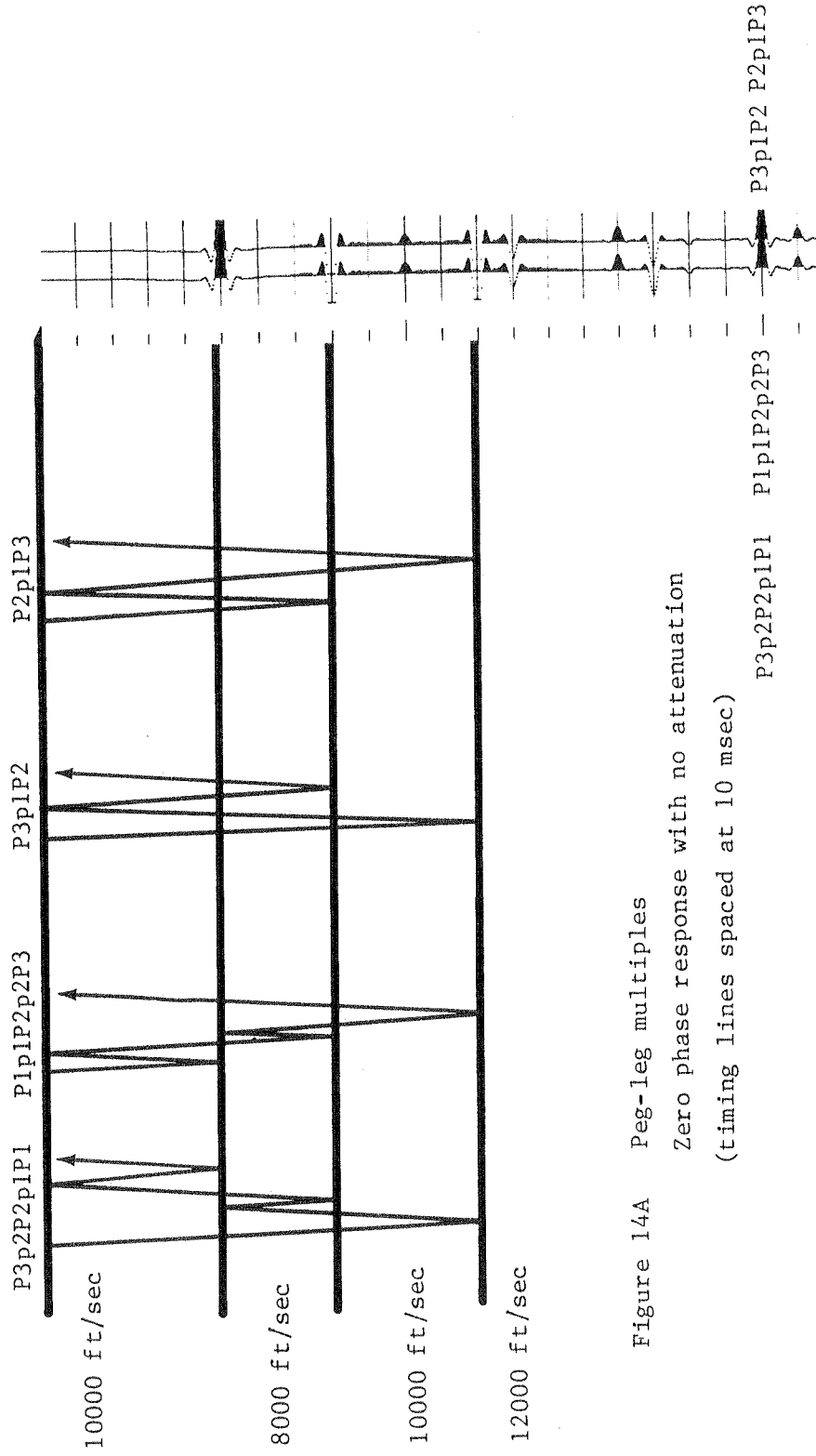


Figure 14A Peg-leg multiples

Zero phase response with no attenuation

(timing lines spaced at 10 msec)

Geologic Model Set 2

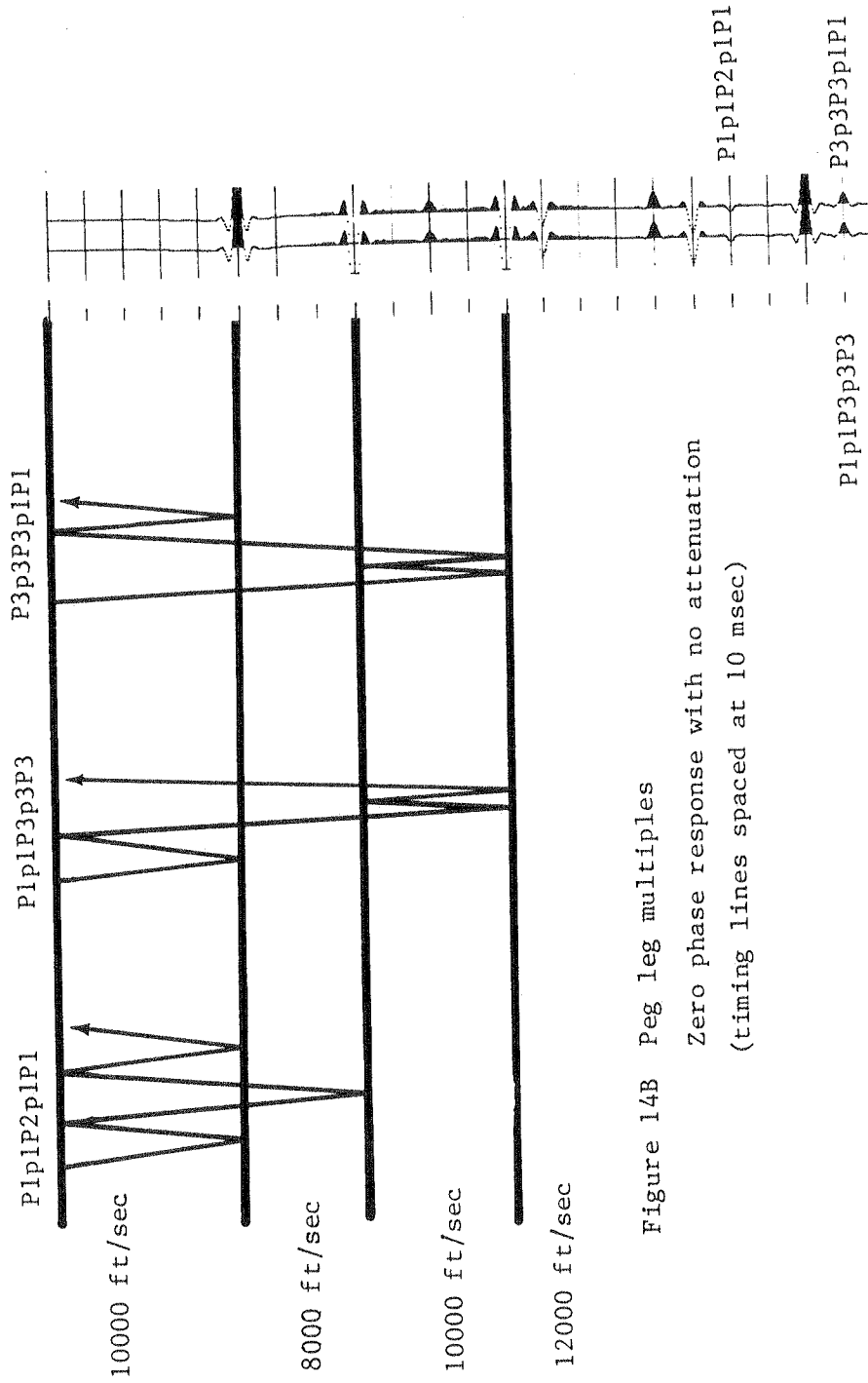


Figure 14B Peg leg multiples

Zero phase response with no attenuation
(timing lines spaced at 10 msec)

MODEL SET 3 - A case study in modeling seismic reflection data

The purpose of this model set is to use SYNSIZE to model real seismic reflection data. A nearby well log yields information on rock layers needed for input to the program, and the output phase shifted response is produced to aid interpretation.

Survey location and method

The reflection survey objective was a sinkhole resulting from dissolution in the 250 foot thick Hutchinson Salt Member of the Wellington Formation near Geneseo, Kansas. Figure 15 shows the location of the lines relative to Kansas and to the sinkhole, respectively. In Miller et. al (1985), the sinkhole is said to result from "dissolution by unsaturated brines from disposal wells or from leakage of surface and/or shallow groundwater alongside well casings."

Two reflection profiles were obtained across the center of the sinkhole. Line 1 consisted of 83 shotpoints occupied at 33 foot intervals, while line two consisted of 84 shot points at 33 foot intervals. This disposition of shotpoints means that the CDP's are spaced at 16.5 foot intervals. Three CDP locations on line 1 are shown in Figure 15.

Geophones were evenly spaced over the shot points; the distance between geophones was approximately three and two-thirds feet. Groups were wired in series with ten geophones per group, each group leading into a single channel on the line.

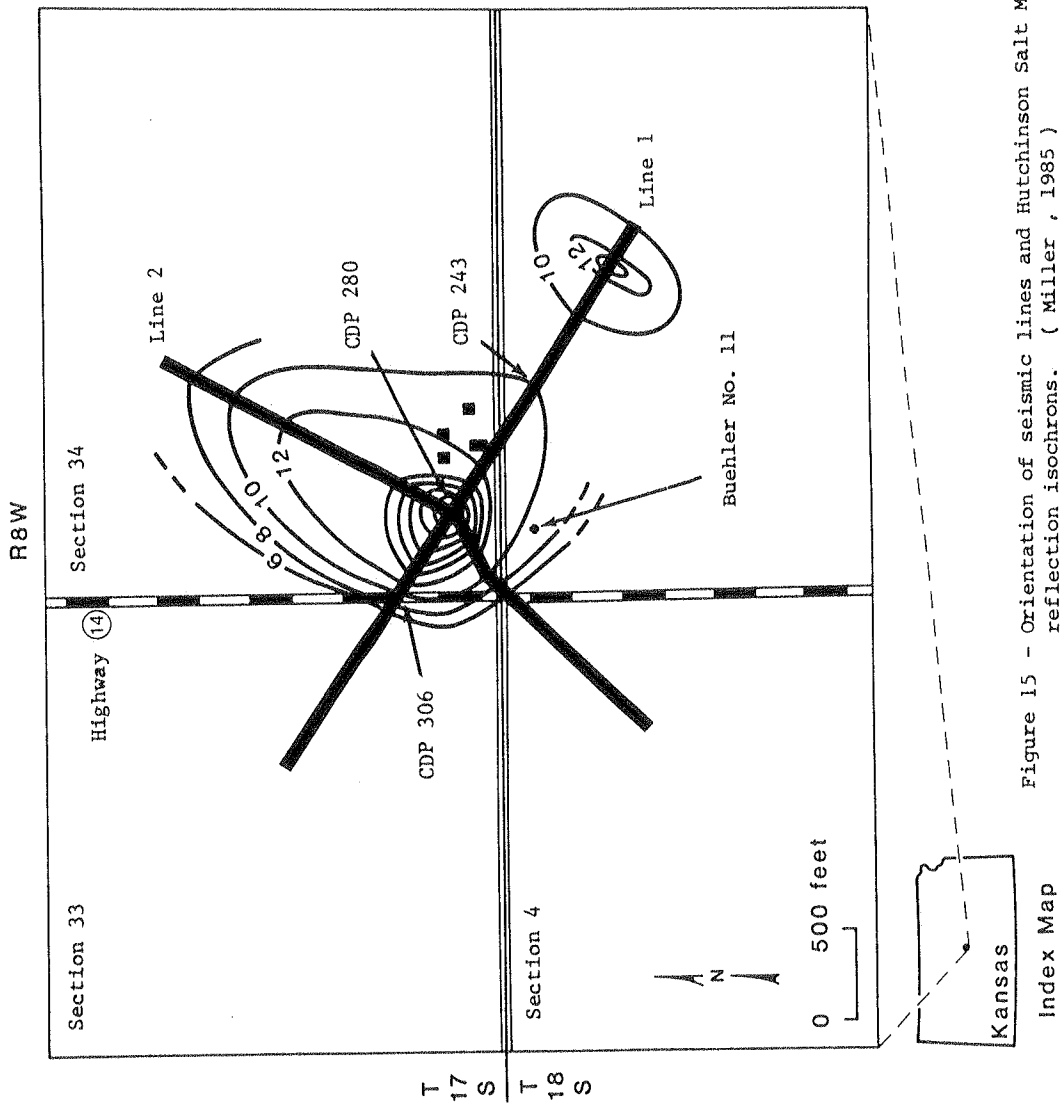


Figure 15 - Orientation of seismic lines and Hutchinson Salt Member reflection isochrons. (Miller , 1985)

The MiniSOSIE method (Barbier, 1976) employed in data recording relies on the random nature in time of the "pops" generated from multiple compactors, since the autocorrelation of the random pop sequence is convolved with the geophone response to produce field files that look like a conventional dynamite record.

Data processing was conducted at the KGS on a Data General 32 bit computer by Dao Somanas, utilizing algorithms from SPEX, a software system developed and marketed by Sytech, Inc. of Houston, Texas.

Geological description

All consolidated rock units relevant to the seismic survey are lower Permian to upper Pennsylvanian in age (Figure 16). Excellent petrologic synopsis of these units is found in Zeller (1968). In brief, the lower Permian section is largely evaporite bearing clastic rocks in the upper two thirds with alternating thin (8 to 40 feet thick) limestones and shales dominating the lower third. Upper Pennsylvanian units were modeled down to the Topeka Limestone, and are characteristically thicker (20 to 60 feet) limestones and shales.

Well control - Gamma and neutron logs

The survey area has been extensively drilled, but many holes have only sketchy "top cards" or "geological reports" completed at the drill site recording the lithologies encountered. The best available information for interpretation of subsurface geology are gamma ray and neutron logs, since shales and sandstones dominate the section. The

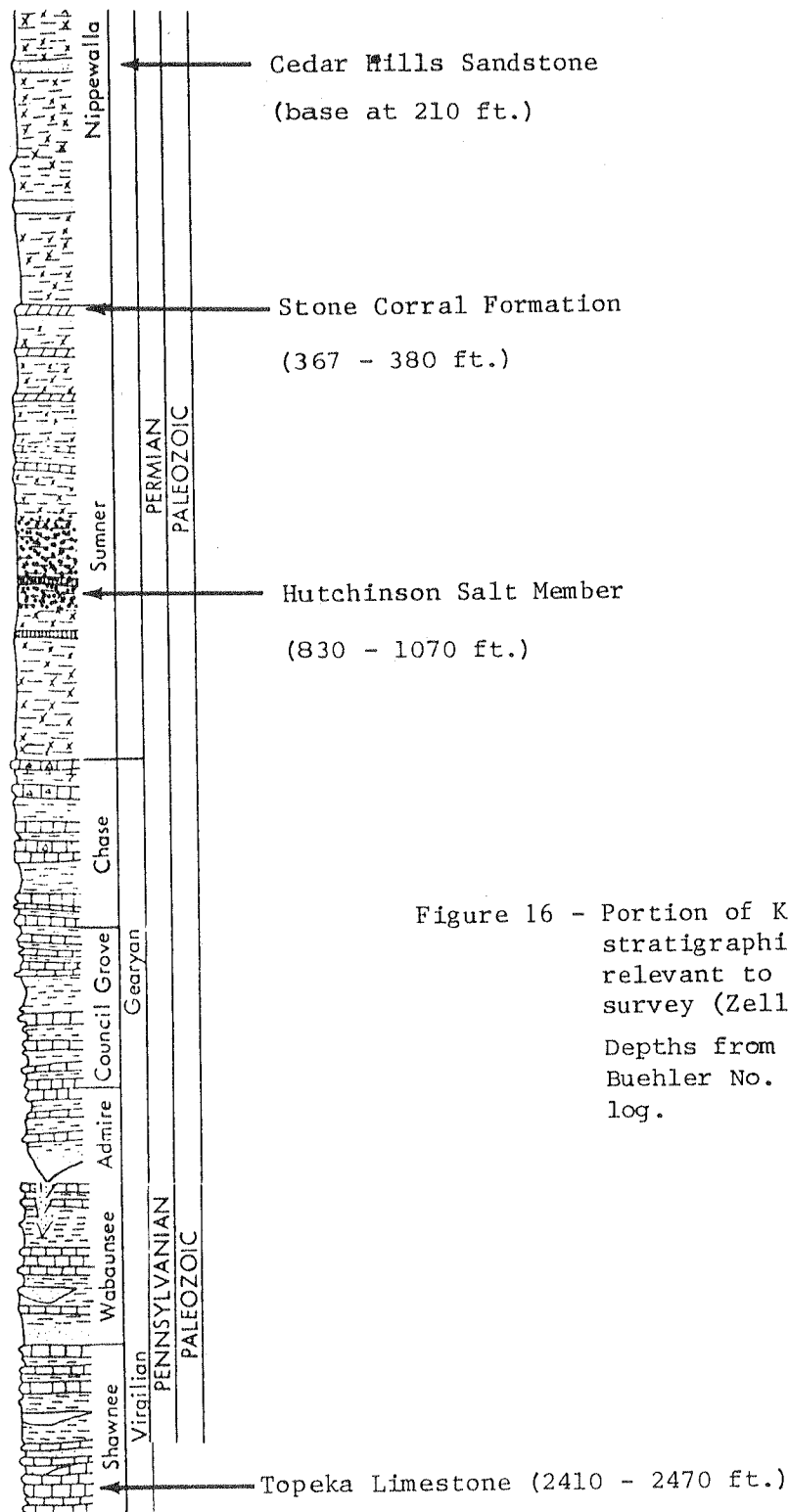


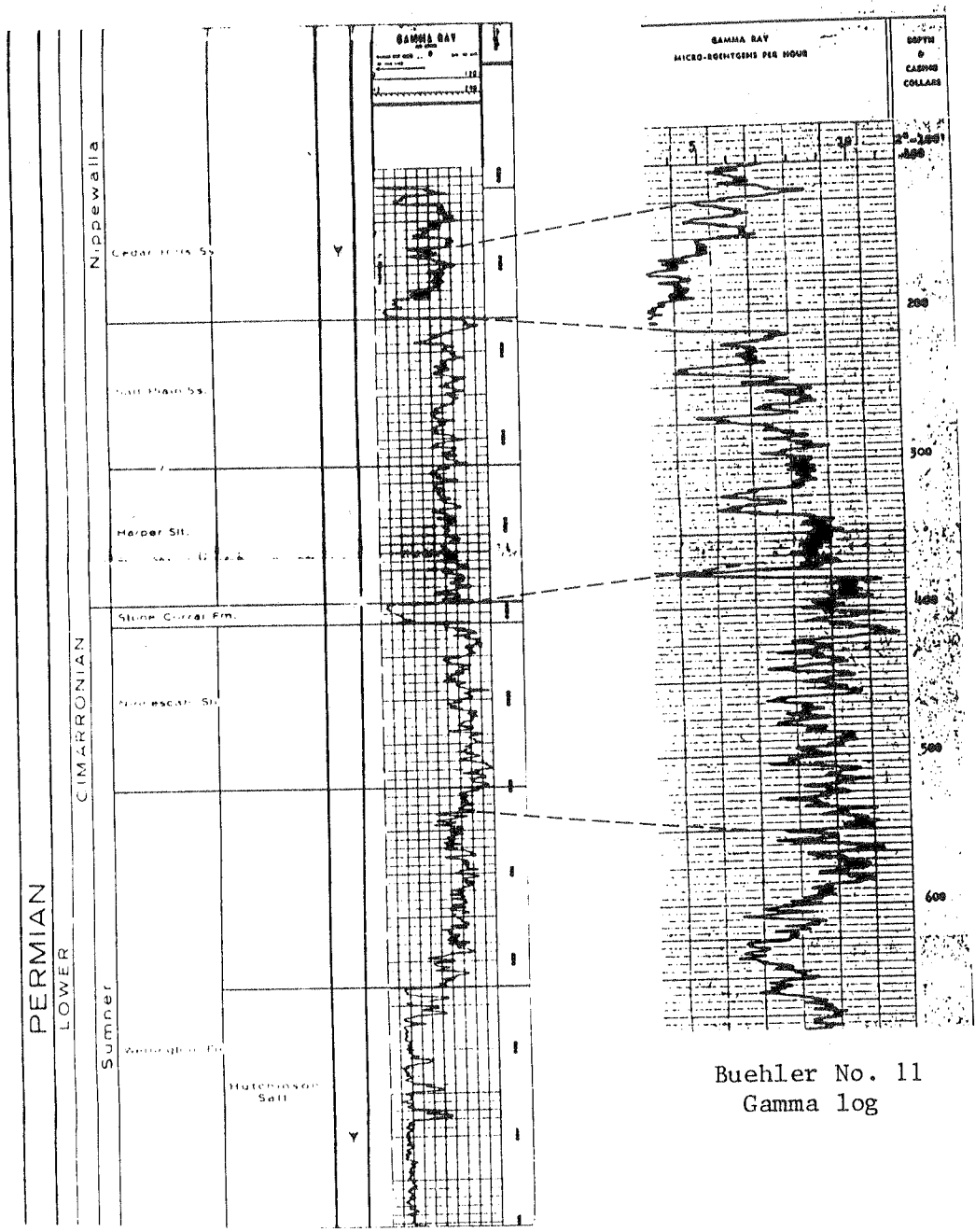
Figure 16 - Portion of Kansas stratigraphic section relevant to the seismic survey (Zeller, 1968)
 Depths from interpreted Buehler No. 11 gamma log.

gamma ray log is highly sensitive to the natural radioactivity of shales, and the neutron log to the hydrogen content and hence the porosity of fluid saturated sandstones.

The chosen logs from Buehler No. 11 (location of this hole is shown on Figure 15) are of high quality and are within 500 feet of the seismic line. These logs were gathered by Perforating Guns Atlas Corp. for Continental Oil Company (Conoco). Type logs from Barton, Ellsworth, and Rice Counties compiled by Harris et al. (1966) also proved invaluable in correlating known lithologies with the gamma and neutron response.

A few observations on the correlation of lithologies are appropriate. Figure 17 shows that the clear identification of the Cedar Hills Sandstone was made largely from an excellent visual match to the gamma-ray response from the Barton County type log. The Stone Corral gives an unmistakable high gamma response, as does the Hutchinson Salt. Interpretation of the thin layers within the Ninnescah shale and the Wellington Formation is not as easy.

Portions of the Wellington above the Hutchinson Salt Member, hereafter referred to as the salt, are dominated by alternating gamma highs and lows, as is the Ninnescah shale. The lithologic differences between these two formations are subtle. Both contain thin, silty sandstone beds. The Ninneschah has thicker shales.



Buehler No. 11
Gamma log

Barton County
Gamma Type log,
from Harris et al.
(1966).

Figure 17 - Comparison of gamma ray logs.

Well control - Sonic logs

No sonic logs within ten miles of the seismic line were available for interpretation. The nearest sonic log was from Rice County, and was completed by Schlumberger for the U.S. Atomic Energy Commission's (AEC) Atomic Waste Repository Project. The log gives interval velocities from the surface to a depth of 1200 feet, roughly one half of the depth to which reflections were recorded. The exact location of the sonic run was in test hole number two, 30' North of Center N/2 of Sec. 35, Twp. 19S, Rge. 8W. This places the sonic run about thirteen miles south of the seismic line.

Modeling process and rock parameters

Rock parameters to be estimated from available data for input to the modeling program SYNSIZE include, for each layer:

- 1) interval velocity,
- 2) thickness,
- 3) density, and
- 4) dissipation factor, (Q).

Parameters one and two are critical in proper time placement of the artificial event relative to the events on the real data. Refraction analysis of the seismic reflection field files produced information on velocities in upper layers. The first breaks of refraction arrivals on the field files were fitted to two lines, corresponding to two layers of velocity 5480 and 7500 feet per second. Interval velocity estimates were made from 120 to 1200 feet by approximating the continuous AEC sonic velocity log with a discontinuous block function. Block lengths were no thinner than five feet and were typically above twenty feet. Blocked log readings were converted from microseconds per foot to interval velocity in feet per second. Interval velocity varied considerably from formation to formation, but showed a high degree of consistency within a given formation. No velocity logs were available below 1200 feet and since 2400 feet of section was modeled, reasonable velocity estimates for lower Permian to upper Pennsylvanian limestones and shales were used from 1200 to 2400 feet.

Interval velocities used in generating the final response were within ten percent of the interval velocity estimates from the sonic log. The tendency of the model velocities to be lower than the sonic velocities by a few percentage points is consistent with a fracture system produced from flexure of the sinkhole beds. Parenthetically, lower seismic model velocities are paralleled by Schenk and Schenkova's (1974) in situ study of the effect of cracks in granodiorite on velocity, where "on an average the presence of cracks decreased the observed wave velocities by 40 percent or more." However, it is likely that sedimentary velocities would be less affected due to the sediments ability to crumble and fill fractures more easily than igneous rock.

Since all modeled units are sedimentary, a reasonable estimation of density based on the lithology is adequate. Reflection coefficients are much less sensitive to density contrasts than to velocity contrasts typically encountered in sedimentary sequences.

Variation in Q was most important for the salt. Salt has a lower Q than other varieties of sedimentary rocks. No direct downhole measurements were available, so Q was estimated from Bradley and Fort (1966) for nonclastics and from a relationship to velocity documented by Waters (1981) for the clastic units (Figure 18).

Interpretation and model results

Two geologic models were generated to fit the observed sinkhole data. The responses for these two models are shown superposed on the

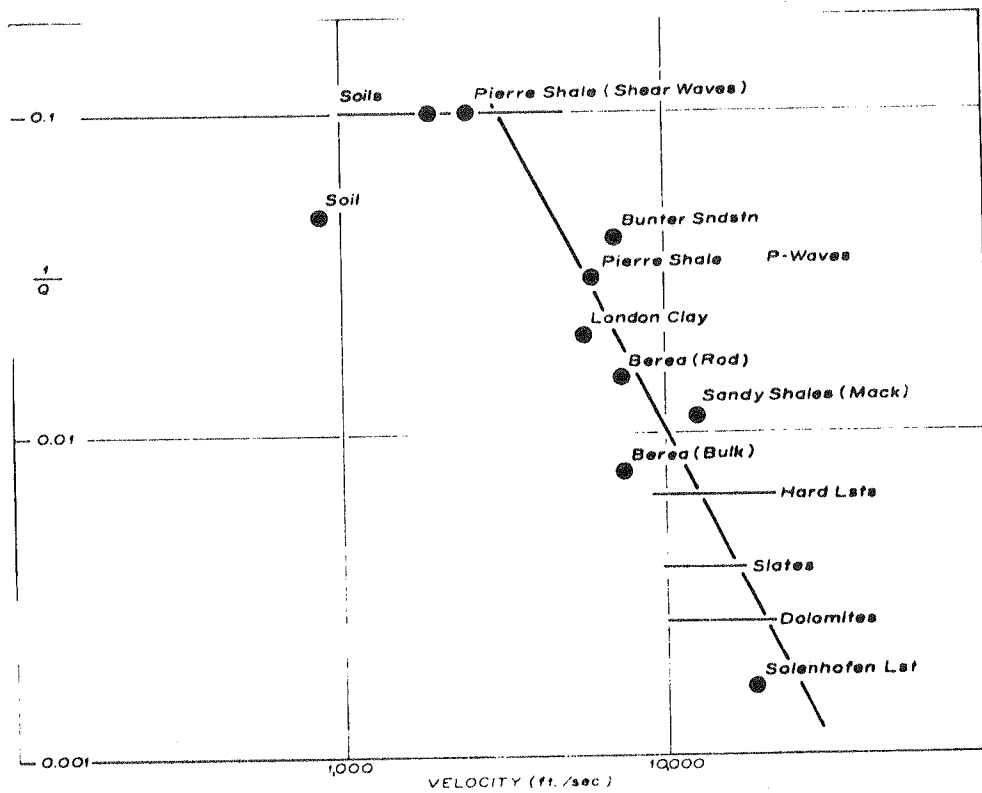


Figure 18 - Q inverse versus velocity, from Waters (1981).

sinkhole data in Figures 19 and 20 respectively, along with important geologic units. The parameters used in generating these synthetic responses are shown in Appendices 2 and 3.

The interpretational starting point for both models was a plausible identification of the event representing the Stone Corral Anhydrite, identified by Glover (1959) as a marker often used in interpreting seismic records in Kansas. Two high amplitude events on the record are the strongest candidates for the Stone Corral. The first occurs at about 110 msec in the center of the sink and the second at about 150 msec in the same position. Both events are laterally continuous and are of high amplitude and coherence relative to other reflections.

The nonuniqueness and subjectivity of modeling geophysical data is demonstrable. Both models result in an acceptable "match" between the synthetic response and the real data. The choice of the second model as the preferred model is based on subjective interpretation elements.

The first of these elements is an examination of amplitude relationships in the real versus the synthetic data sets for the four coherent events between 100 and 160 msec in the sink's center. The amplitude pattern for these four events is more closely matched to the real data by model 1; the events over this time window in model 1 do not demonstrate a similar variation in amplitude. At this point, one might raise the question of amplitude distortion due to the application of automatic gain control. The counter argument is that the AGC

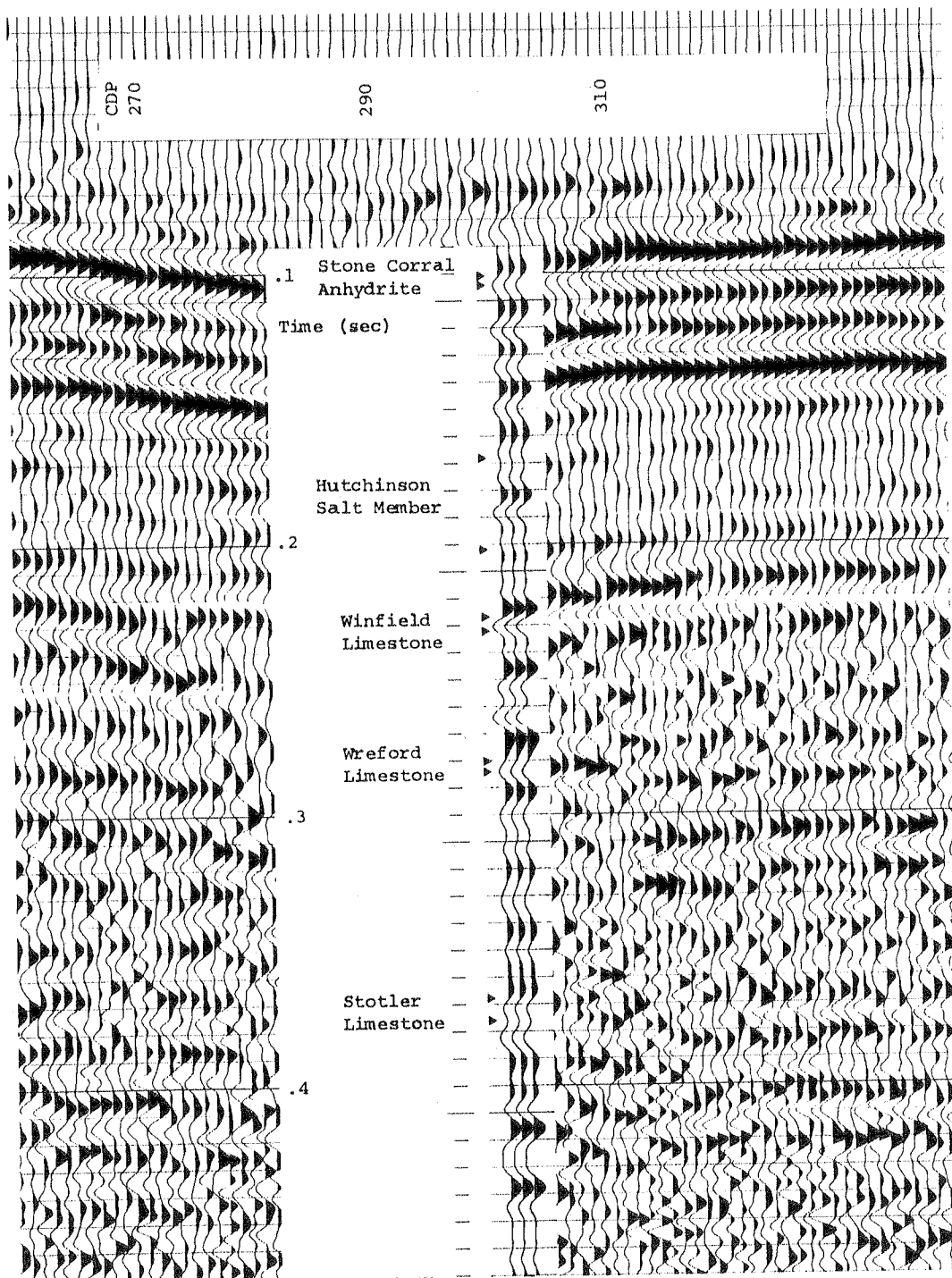


Figure 19 - Model 1.
 Comparison of sinkhole data and synthetic data.
 (Parameters for synthetic data shown in Appendix 2.)

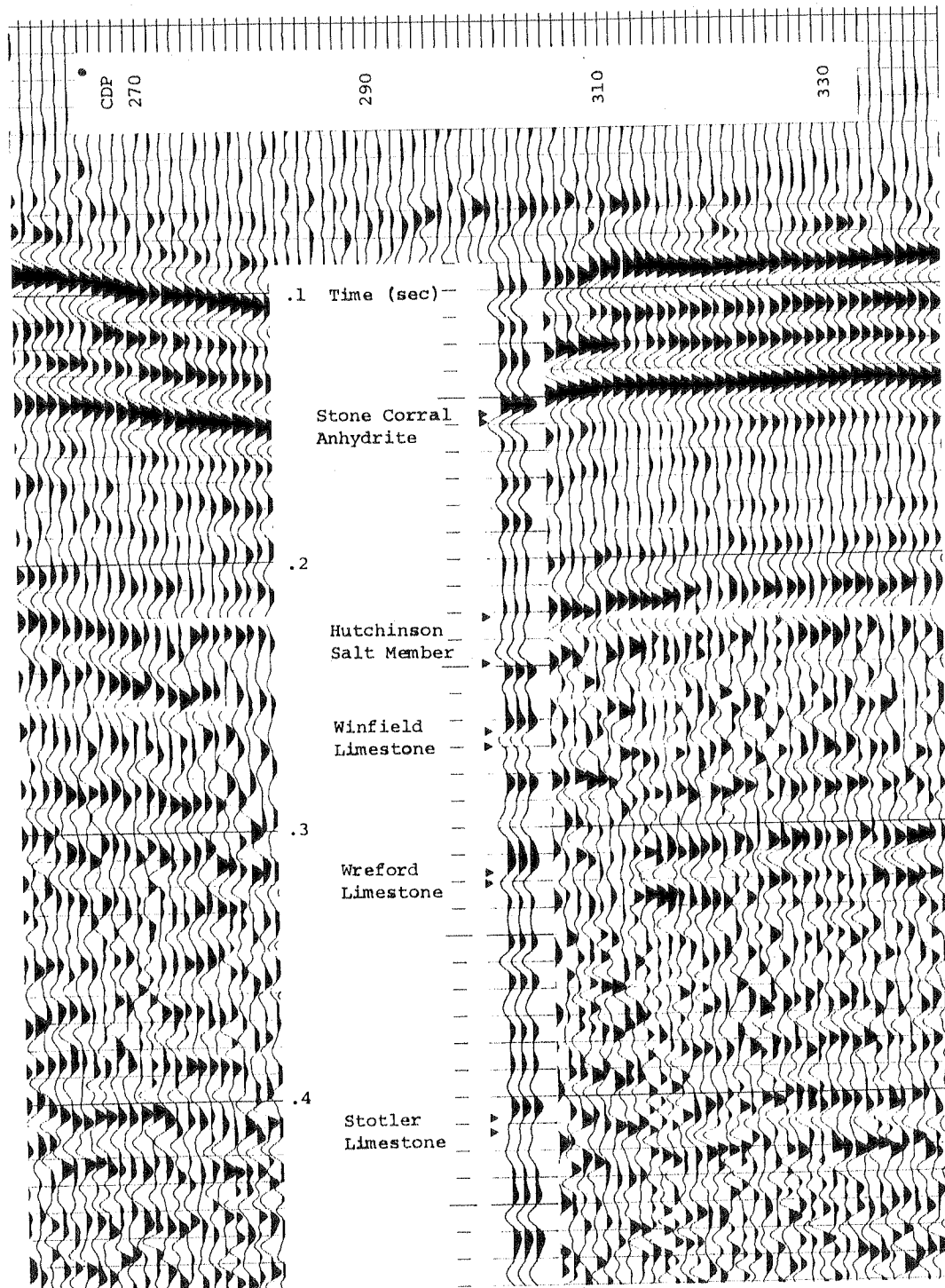


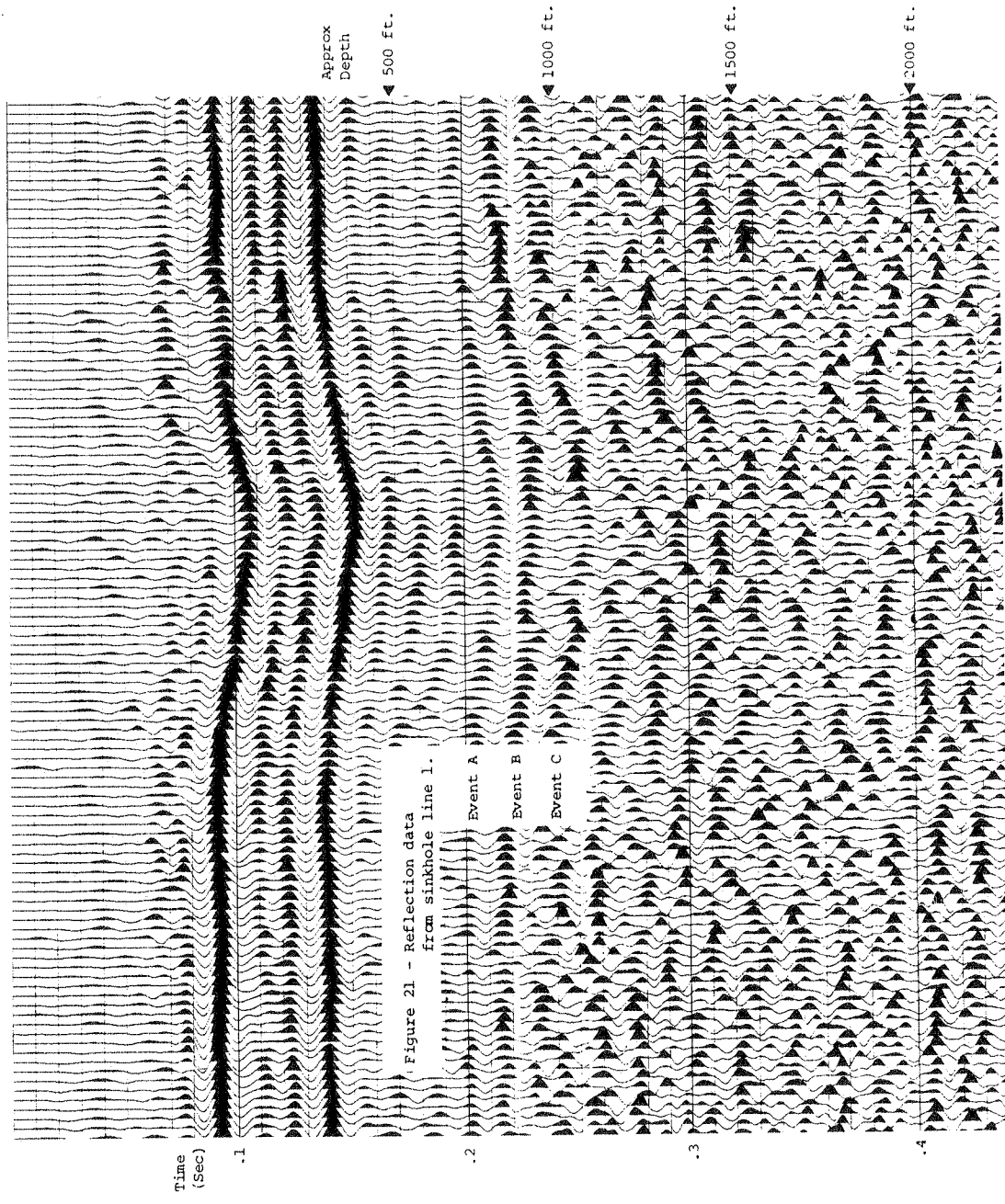
Figure 20 - Model 2.
 Comparison of sinkhole data and synthetic data.
 (Parameters for synthetic data shown in Appendix 3.)

window was of sufficient length (150 msec for both the real and simulated data) to disallow gross distortion of events relative to one another within the 60 msec window over which amplitudes are compared.

The second element favoring model 2 is successful interpretation of the data based on a conceptual model of the sink, i.e. that the sinkhole resulted from dissolution of the salt member, and that successful interpretation of the data should support salt dissolution as the cause for the sink. Model 1 falls short in that the events corresponding to the salt lie within a zone of weak reflection amplitudes between 160 and 200 msec and show none of the effects anticipated from dissolution. One would expect fairly strong events on the record corresponding to the top and/or the base of the salt, since the velocity contrast of the salt relative to surrounding units is substantial on the sonic logs. Instead in model 1 the salt zone is not delineated by strong events. This is true on the data as well, and is not consistent with the reasonable expectation of a higher amplitude event anticipated from a salt/clastic contact. Model 2, however, shows strong events at the top and at the base of the salt, corresponding to events observed on the real data. Examination of the model parameters in Appendices 1 and 2 show comparable velocity contrasts for the salt/clastic contacts in both model runs. The lower amplitude of the salt contacts in model 1 might be attributed to the destructive interference of primary and multiple energy in the 160 to 200 msec zone. Peg-leg multiples from the Stone Corral could arrive within this time window.

Lastly, the zone on the seismic section correlating with the salt of model 1 demonstrates no thinning or thickening of the salt contact events as one traverses the sink. This is inconsistent with the notion that either i) thickening due to a velocity decrease from fracturing and/or ii) thinning due to dissolution of the salt or disintegration of overlying strata should be present on the record and associated with the salt. Both of these phenomena are present in the model 2 salt zone. The zone between events A and B shown in Figure 21 thins from 20 msec on the rim of the sink to about 15 msec in the center. The zone between events B and C thickens from 18 msec on the rim to 25 msec or so in the center. While interpretation of this behavior is subjective, the decrease of coherence in event C as one traces this event into the center of the sink and the thickening between events B and C might be attributable to a rubble zone above the partially dissolved salt. Fractures in such a zone would i) lower the velocity and produce the observed thickening, and ii) lower the coherence of reflected energy due to their nonuniformity.

Thinning effects might be explained above the dissolved zone if one views the "void" created by dissolution and the permeation of groundwater in the the strata above the salt as sufficient cause for increased compaction. This would produce velocity and/or thickness changes in the center of the sink.



Conclusions: Model Set 3

The program SYNSIZE may serve as an interpretational aid to seismic interpretation of stacked CDP data. In addition the normal incidence approximation of CDP data resulting from the iterative solution of the one dimensional wave equation is justifiable in that;

i) a reasonable fit to stacked CDP data is obtained.

ii) CPU time necessary for computation of the response is a few minutes per run, expediting the successive refinement of models.

Although difficult to quantify;

iii) the inclusion of pulse broadening in the program did not hinder the production of a synthetic multiple layer product that fits the real data. This is desirable since seismic waves are more accurately simulated if frequency dependent attenuation is included.

GENERAL CONCLUSION

The process of accurately modeling real CDP data in Kansas iteratively with minimum computer time requires the use of an efficient program simulating the response from dozens of thin layers. In Kansas, wide offsets are not typically employed in CDP surveys, and geologic structures that might be modeled are typified by gentle synclines, anticlines, folds or normal faults. This makes the normal incidence approximation of SYNSIZE appropriate. In these cases, modeling a few CDP's at various locations in the line, in lieu of simulating the response of the total structure, is helpful in relating observed reflections to known rock layers. This became evident in Model Set 3 when one of two proposed models emerged in the light of geologic interpretation consistent with salt dissolution as the cause for the sinkhole.

Linear frequency dependent attenuation is supported by Kjartansson's (1979) review of 25 attenuation papers. This attenuation model is easily introduced if calculations are performed in the frequency domain. A visual comparison of the synthetic traces from Model 3 with the real data shows that the synthetic data closely approximate real data when frequency dependent attenuation is included.

REFERENCES

- Aki, K., and Richards, P.G., 1980, Quantitative seismology, theory and methods: W.H. Freeman and Company.
- Barbier, M.G., 1976, MiniSOSIE for land seismology, Geophysical Prospecting, 24, 518.
- Bland, D.R., 1960, The theory of linear viscoelasticity: Pergamon, New York.
- Bradley, J.J., and Fort, A.N. Jr., 1966, Internal friction in rocks, in Clark, S.P. Jr., ed., 1966, Handbook of Physical Constants: GSA Publications.
- Brennan, B.J., and Stacey, F.D., 1977, Frequency dependence of elasticity of rock- test of seismic velocity dispersion, Nature, 268, 220-222.
- Claerbout, J.F., and Riley, D.C., 1976, "2-d multiple reflections, Geophysics, 41, 592-620.
- Dobrin, M.B., 1976, Introduction to geophysical prospecting: McGraw Hill.
- Ellsworth, T.P., 1948, Multiple reflections, Geophysics, 13, 1-18.
- Garland, G.D., 1979, Introduction to geophysics, mantle core and crust: W.B. Saunders Company.
- Glover, R.H., 1959, Techniques used in interpreting seismic data in Kansas, Symposium on Geophysics in Kansas, ed. Hambleton, W.W., Univ. of Kansas publications, State Geological Survey of Kansas, Bulletin 137.

- Harris, R.L., Stone, J.J., King, C.R., James, A. III, Goebel, E.D.,
1966, Type logs of Kansas, Kansas Geological Society, Wichita,
Kansas.
- Johnson, D.H., and Toksoz, M.N., 1981, Seismic wave attenuation,
Geophysics reprint series 2: Society of Exploration
Geophysicists, 352.
- Kallweit, R.S., and Wood, L.C., 1982, The limits of resolution of zero
phase wavelets, Geophysics, 47, 1035-1046.
- Kennett, B.L.N., 1978, Theoretical reflection seismograms for elastic
media, Geophysical Prospecting, 27, 301-321.
- Kjartansson, E., 1979, Constant Q wave propagation and attenuation,
Journal of Geophysical Research, 84, 4737-4748.
- McDonal, F.J., Angona, F.A., Mills, R.R., Sengbush, R.L., von
Nostrand, R.G., White, J.E., 1958, Attenuation of shear and
compressional waves in Pierre Shale, Geophysics, 23, 421-439.
- Miller, R.D., Steeples, D.W., Treadway, J.A., 1985, Seismic reflection
survey of a sinkhole in Ellsworth County, Kansas, accepted
Society of Exploration Geophysicists Annual Meeting, October 7-11,
Washington, D.C.
- Morrison, J., 1984, Verbal communication, Senior Geophysicist, Chevron
U.S.A, New Orleans, La.
- Peterson, R.A., Fillipone, W.R., Coker, F.B., 1955, The synthesis of
seismograms from well log data, Geophysics 26, 138-150.
- Ricker, N., 1953, The form and laws of propagation of seismic
wavelets, Geophysics, 18, 10-40.

- Robinson, E.A., and Trietel, S., 1980, Geophysical signal analysis:
Prentice-Hall Inc.
- Schenk, V. and Schenkova, 1974, Stress wave velocity and crack system
of a medium, Geophysical Prospecting, 22, 710-721.
- Schoenberger M., and Levin, F.K., 1974, Apparent attenuation due to
intrabed multiples, Geophysics, 39, 278-291.
- Sheriff, R.E., ed., 1984, Encyclopedic dictionary of exploration
geophysics, Society of exploration geophysicists.
- Strick, E., 1967, The determination of Q, dynamic viscosity and creep
curves from wave propagation measurements, Geophysical Journal of
the Royal Astronomical Society, 197-218.
- Thompson, W.T., 1950, Transmission of elastic waves through a
stratified solid medium, Journal of Applied Physics, 21, 89-93.
- Tooley, R.D., Spencer, T.W., Sagoci, H.F., 1965, Reflection and
transmission of plane compressional waves, Geophysics, 30, 552-
570.
- Trorey, A.W., 1962, Theoretical seismograms with frequency and depth
dependent absorption, Geophysics, 27, 766-775.
- Van Melle, F.A., and Weatherburn, K.R., 1953, Ghost reflections caused
by energy initially reflected above the level of the shot,
Geophysics, 18, 793-804.
- Waters, K.H., 1981, Reflection seismology: a tool for energy resource
exploration, John Wiley and Sons, Inc.
- Widess, M.B., 1973, How thin is a thin bed?, Geophysics, 38, 1176-
1185.

Widess, 1982, Quantifying resolving power of seismic systems,
Geophysics, 47, 1760-1765.

Wuenschel, P.E., 1960, Seismogram synthesis including multiples and
transmission coefficients, Geophysics, 25, 106-129.

Zeller, D.E., 1968, The stratigraphic succession in Kansas, Kansas
Geological Survey Bulletin 189.

Appendix 1 - Fortran 77 code for the program, SYNSIZE.

) TY SYNEX

SYNSIZE AUTHOR:G.W. NEELY MAY 15,1985

A PROGRAM DESIGNED TO CALCULATE SEISMIC RESPONSES
IN THE FREQUENCY DOMAIN FOR FLAT LYING LAYERS.

THE FINAL PROGRAM OUTPUT IS DISPLAYED AS A TIME DOMAIN
SEISMIC TRACE INCLUDING TRANSMISSION EFFECTS I.E. PEG-LEG
AND SHORT PATH MULTIPLES.

THE PROGRAM IS BASED ON AN ALGORITHM DISCUSSED IN DETAIL
IN THE TEXT, REFLECTION SEISMOLOGY: A TOOL FOR ENERGY
RESOURCE EXPLORATION, KENNETH H. WATERS, 1981, JOHN WILEY
AND SONS., P. 148.

THE USER SETS UP AN INPUT FILE CONTAINING THE VALID PARAMETERS
OF LAYER THICKNESS, VELOCITY, AND Q VALUES. Q VALUES ARE
SOMETIMES CALLED SPECIFIC LOSS FACTORS.

AN EXAMPLE OF AN INPUT FILE MIGHT BE:

```
3
200.,8000.,2.2,10.
50.,12000.,2.4,20.
40.,10000.,2.67,80.
20000.,2.5,40.
.00025
1
10
90
.5
```

THE RELATIONSHIP OF THE ABOVE INFORMATION TO A GEOLOGIC MODEL
IS SHOWN IN THE FIGURE BELOW. Q VALUES DOCUMENTED IN THE
LITERATURE RANGE FROM 10 IN A VERY ATTENUATIVE SHALE
TO 500 FOR SOME GRANITES.

WATERS GIVES AN EMPIRICAL RELATIONSHIP BETWEEN COMPRESSIONAL
VELOCITY AND Q:

$$Q=(VELOCITY **2)/(10**6) \quad \text{IN ENGLISH UNITS.}$$

THIS SHOULD GET ONE "OFF THE GROUND" AND MODELING.

-----SURFACE		
DENSITY=2.2	Q=10	
VELOCITY=8000		
-----		INTERFACE 1 (200 FT)
		DEPTH 200 FT.
DENSITY=2.4	Q=20	
VELOCITY=12000		
-----		INTERFACE 2 (50 FT)
		DEPTH 250 FT.
DENSITY=2.67	Q=80	
VELOCITY=10000		
-----		INTERFACE 3 (40 FT)
		DEPTH 290 FT.
DENSITY=2.5	Q=40	
VELOCITY=20000		

INTEGER '3' AT THE BEGINNING OF THE DATALIST REPRESENTS
THREE BOUNDED LAYERS SYNONYMOUS WITH 3 ACTIVE
INTERFACES IN THE MODEL. UP TO 49 BOUNDED LAYERS MAY BE
SPECIFIED.


```

DO 53 JJJ=1,ULT
  W(JJJ)=1.0
53 CONTINUE
C
C THIS GIVES PI TO HIGH ACCURACY.
C
C PI=ATAN(1.0)*4
C
DO 54 KKK=SUL,UI.
  W(KKK)=.5 + (.50)*COS(PI*(KKK-2048)/2048)
54 CONTINUE
C
C
C WRITE(18,*)"*****"
C WRITE(18,*)"PROGRAM OUTPUT-----SYNSIZE  AUTHORS:G.W. NEELY"
C WRITE(18,*)"KANSAS GEOLOGICAL SURVEY          C. MCFI WFE"
C WRITE(18,*)"CODE COMPLETED JULY 1, 1985      R.W. KNAPP"
C WRITE(18,*)"*****"
C
C DETERMINE TWO WAY INTERVAL TIME FOR EACH LAYER AND
C CUMULATIVE TWO WAY TRAVEL TIME TO THE BASE OF EACH
C LAYER AND DISPLAY.
C
C DEPTH=0.0
C TCUM=0.0
C
C WRITE(18,*)"LAYER THICKNESS DEPTH VELOCITY 2-WAY CUMULATIVE"
C WRITE(18,*)" TRAVEL TIME (MS)"
C
C DO 77 I=1,NUM
C   T2WAY(I)=(X(I)*2000.)/VELS(I)
C   TCUM=TCUM+T2WAY(I)
C   DEPTH=DEPTH+X(I)
C
C PRINT OUT TRAVEL TIME INFORMATION.
C
C WRITE(18,921)I,X(I),DEPTH,VELS(I),TCUM
C   FORMAT(1X,I2,6X,F5.1,6X,F6.1,6X,F7.0,7X,F5.1)
921 CONTINUE
C
C WRITE(18,*)"*****"
C
C OBTAIN 'E' TO HIGH ACCURACY
C
C Y=2.7182818284959045
C
C
C CALCULATE THE PROPER FREQUENCY INCREMENT FOR INVERSE
C DISCREET FOURIER TRANSFORM.
C THIS IS NECESSARY SINCE THE RESPONSE IS GENERATED IN THE
C FREQUENCY DOMAIN. THE BANDPASS OF THE RESPONSE MUST BE
C SPECIFIED. THIS IS DONE AUTOMATICALLY BY THE PROGRAM.
C THE BANDPASS IS SPLIT INTO INCREMENTS OF WIDTH FINC WHERE
C
C FINC=(1.0)/(SAMN*SINT)
C
C THE BANDPASS IS FROM OMEGA(1)-ZERO FREQUENCY-- TO OMEGA(2049)--
C THE NYQUIST FREQUENCY.
C
C THE ANGULAR FREQUENCY INCREMENT IS
C
C OINC=2.0*PI*FINC

```

```

C
C
C      EXPRESS THE SAMPLE INTERVAL IN SAMPLES PER MICROSECOND.
C
C      SR=INT(SINT*1000000)
C
C      SUBDIVIDE THE BANDWIDTH INTO SEGMENTS AND LOAD ARRAY OMEGA
C      CONTAINING EACH ANGULAR FREQUENCY FOR WHICH RESPONSE IS CAL-
C      CULATED.
C
C      OMEGA(1)=0.0
C      DO 5 I=2,UL
C          OMEGA(I)=(I-1)*OINC
5      CONTINUE
C      WRITE(18,*)'THE IMPULSE RESPONSE HAS BEEN CALCULATED FROM'
C      WRITE(18,*)'ANGULAR FREQUENCY ',-OMEGA(UL),' TO ANGULAR'
C      WRITE(18,*)'FREQUENCY ',OMEGA(UL)
C
C      THE CALLS ON THE FOLLOWING NAMED SUBROUTINES ARE NESTED
C      INSIDE OF A DO LOOP AND MUST BE CALLED FOR EACH ANGULAR
C      FREQUENCY.
C
C      THE RESULT OF EACH PASS THROUGH THE LOOP IS A SINGLE COMPLEX
C      VALUE , 'AMPRT'. 'AMPRT'S REAL PART IS USED IN A SIMPLE
C      FORMULA TO OBTAIN SEISMIC AMPLITUDE.
C
C      DO 8 M=1,UL
C
C      CALCULATE THE ATTENUATION COEFFICIENT
C      FOR EACH LAYER.
C
C      SET FLAG TO ONE IF AT MAXIMUM FREQUENCY
C
C      IF(M.EQ,UL)THEN
C          INDI=1
C      ELSE
C          INDI=0
C      ENDIF
C
C      CALL ATTENU(NUM,OMEGA(M),VELS,QUE,ACDEF,ZU,QOP,INDI,ULAC)
C
C      GIVE THE VALUE OF THE ATTENUATION COEFFICIENT AT THE
C      LOW AND HIGH END WITHIN THE DESIGNATED BANDPASS.
C
C      IF (OMEGA(M).EQ,OMEGA(1))THEN
C          WRITE(18,*)'*****'
C          WRITE(18,*)'THE ATTENUATION COEFFICIENT FOR THE'
C          WRITE(18,*)'LAYERS FOR ANGULAR FREQUENCY ',OMEGA(1)
C          WRITE(18,*)'*****'
C          IF(NUM.GT,1)THEN
C              WRITE(18,*)'UPPERMOST LAYER ',ACDEF(1)
C              DO 12 K=2,NUM
C                  WRITE(18,*)'BOUNDED LAYER ',K,' ',ACDEF(K)
12          CONTINUE
C              WRITE(18,*)'LOWER HALF SPACE ',ACDEF(NUM+1)
C          ELSE
C              WRITE(18,*)'SINGLE BOUNDED LAYER ',ACDEF(1)
C              WRITE(18,*)'LOWER HALF SPACE ',ACDEF(2)
C          ENDIF
C      ELSE
C          ENDIF
C
C      ENDIF
C

```

```

C
IF (OMEGA(M).EQ.OMEGA(UL))THEN
WRITE(18,*)"*****"
WRITE(18,*)"THE ATTENUATION COEFFICIENT FOR THE"
WRITE(18,*)"LAYERS FOR ANGULAR FREQUENCY ",OMEGA(UL)
WRITE(18,*)"*****"
IF(NUM.GT.1)THEN
WRITE(18,*)"UPPERMOST LAYER ",ACOFF(1)
DO 21 K=2,NUM
WRITE(18,*)"BOUNDED LAYER ",K," ",ACOFF(K)
21 CONTINUE
WRITE(18,*)"LOWER HALF SPACE ",ACOFF(NUM+1)
ELSE
WRITE(18,*)"SINGLE BOUNDED LAYER ",ACOFF(1)
WRITE(18,*)"LOWER HALF SPACE ",ACOFF(2)
ENDIF
ELSE
ENDIF
ENDIF

C
C
C
C
CALCULATE THE RATIO OF COMPLEX ACOUSTIC IMPEDANCES FOR EACH
INTERFACE.
CALL AIRAT(VELS,ZU,RHO,NUM,KAY)

C
C
IF(OMEGA(M).EQ.OMEGA(1))THEN
WRITE(18,*)"*****"
WRITE(18,*)"THE COMPLEX ACOUSTIC IMPEDENCE RATIOS FOR"
WRITE(18,*)"EACH INTERFACE FOR ANGULAR FREQUENCY ",OMEGA(1)
WRITE(18,*)"*****"
IF(NUM.GT.1)THEN
WRITE(18,*)"BASE OF UPPERMOST LAYER ",KAY(1)
DO 18 J=1,NUM
WRITE(18,*)"BASE OF BOUNDED LAYER ",J," ",KAY(J)
18 CONTINUE
ELSE
WRITE(18,*)"BASE OF SINGLE BOUNDED LAYER ",KAY(1)
ENDIF
ELSE
ENDIF
ENDIF

C
IF(OMEGA(M).EQ.OMEGA(UL))THEN
WRITE(18,*)"*****"
WRITE(18,*)"THE COMPLEX ACOUSTIC IMPEDENCE RATIOS FOR"
WRITE(18,*)"EACH INTERFACE FOR ANGULAR FREQUENCY ",OMEGA(UL)
WRITE(18,*)"*****"
IF(NUM.GT.1)THEN
WRITE(18,*)"BASE OF UPPERMOST LAYER ",KAY(1)
DO 81 J=2,NUM
WRITE(18,*)"BASE OF BOUNDED LAYER ",J," ",KAY(J)
81 CONTINUE
ELSE
WRITE(18,*)"BASE OF SINGLE BOUNDED LAYER ",KAY(1)
ENDIF
ELSE
ENDIF
ENDIF

C
C
C
C
CALCULATE THE COMPLEX REFLECTION COEFFICIENT FOR EACH
INTERFACE.
CALL CREFCO(NUM,KAY,REFCO)

```

```

C
IF(OMEGA(M).EQ.OMEGA(1))THEN
WRITE(18,*)"*****"
WRITE(18,*)"THE COMPLEX REFLECTION COEFFICIENT FOR EACH"
WRITE(18,*)"INTERFACE FOR ANGULAR FREQUENCY ",OMEGA(1)
WRITE(18,*)"*****"
IF(NUM.GT.1)THEN
WRITE(18,*)"BASE OF UPPERMOST LAYER ",REFCO(1)
DO 19 L=2,NUM
WRITE(18,*)"BASE OF BOUNDED LAYER ',L,' ',REFCO(L)
19 CONTINUE
ELSE
WRITE(18,*)"BASE OF SINGLE BOUNDED LAYER ',REFCO(1)
ENDIF
ELSE
ENDIF

```

```

C
IF(OMEGA(M).EQ.OMEGA(UL))THEN
WRITE(18,*)"*****"
WRITE(18,*)"THE COMPLEX REFLECTION COEFFICIENT FOR EACH"
WRITE(18,*)"INTERFACE FOR ANGULAR FREQUENCY ",OMEGA(UL)
WRITE(18,*)"*****"
IF(NUM.GT.1)THEN
WRITE(18,*)"BASE OF UPPERMOST LAYER ",REFCO(1)
DO 91 L=2,NUM
WRITE(18,*)"BASE OF BOUNDED LAYER ',L,' ',REFCO(L)
91 CONTINUE
ELSE
WRITE(18,*)"BASE OF SINGLE BOUNDED LAYER ',REFCO(1)
ENDIF
ELSE
ENDIF

```

```

C
C
C
C
C
C
C
C
NOW WE FIND THE RATIO OF THE AMPLITUDE OF THE UP
TRAVELING WAVE TO THAT OF THE DOWN TRAVELING WAVE FOR THE
LOWEST BOUNDED LAYER OF THE STRATIGRAPHIC SEQUENCE.

```

```

C
CALL START(REFCO,X,ACDEF,VELS,OMEGA(M),NUM,SEED)
IF(OMEGA(M).EQ.OMEGA(1))THEN
WRITE(18,*)"*****"
WRITE(18,*)"THE RATIO OF UP TO DOWN TRAVELING WAVE"
WRITE(18,*)"AMPLITUDES (AMPRAT) NEAR THE TOP OF THE LOWEST"
WRITE(18,*)"BOUNDED LAYER FOR ANGULAR FREQUENCY ",OMEGA(1)
WRITE(18,*)"*****"
WRITE(18,*)SEED
ELSE
ENDIF

```

```

C
IF(OMEGA(M).EQ.OMEGA(UL))THEN
WRITE(18,*)"*****"
WRITE(18,*)"THE RATIO OF UP TO DOWN TRAVELING WAVE"
WRITE(18,*)"AMPLITUDES (AMPRAT) NEAR THE TOP OF THE LOWEST"
WRITE(18,*)"BOUNDED LAYER FOR ANGULAR FREQUENCY ",OMEGA(UL)
WRITE(18,*)"*****"
WRITE(18,*)SEED
ELSE
ENDIF

```

```

C
C
C
C
C
C
C
C
NOW OBTAIN A CUMULATIVE RATIO OF THE UPCOMING
TO DOWNGOING WAVE AMPLITUDES AT THE SURFACE,
STARTING AT THE BOUNDED LAYER NEXT UP FROM THE
BOTTOM BOUNDED LAYER USING THE "SEED" VALUE CALCULATED
FROM SUBROUTINE START.

```

```

C
C
C      SUBROUTINE CARAT IS NOT NEEDED IF THERE IS ONLY ONE
C      REFLECTING HORIZON.
C
C      IF(NUM.GT.1)THEN
C
C          LO=OMEGA(1)
C          HI=OMEGA(UL)
C
C          CALL CARAT(NUM,REFCO,ACOFF,X,VELS,OMEGA(M),SEED,LO,HI,
1      AMPRAT)
C
C          ELSE
C          AMPRAT=SEED
C          ENDF
C
C          DETERMINE FINAL OUTPUT FOR A GIVE FRQUENCY OMEGA.
C          AND STORE IN ARRAY FOUT
C
C          FOUT(M)=AMPRAT/(AMPRAT-1)
C
C          CONTINUE
C
C          MULTIPLY THE DATA TIMES A HANNING WINDOW.
C
C          DO 55 LLL=2,UL
C              FOUT(LLL)=W(LLL)*FOUT(LLL)
55      CONTINUE
C
C          NOW TAKE THE COMPLEX CONJUGATE AND LOAD INTO A MIRROR ARRAY.
C
C          SUD=UL-2
C
C          DO 17 NNN=1,SUD
C              TUOF(NNN)=FOUT(UL-NNN)
17      CONTINUE
C              III=1
C
C          DUS=UL+1
C
C          DO 93 LLL=DUS,SAMN
C              FOUT(LLL)=TUOF(III)
C              III=III+1
C              RFOUT=REAL(FOUT(LLL))
C              IFOUT=-AIMAG(FOUT(LLL))
C              FOUT(LLL)=CMPLX(RFOUT,IFOUT)
93      CONTINUE
C
C          APPLY THE DESIRED PHASE SHIFT
C
C          IF(PHASER.NE.0.)THEN
C              WRITE(18,*)'PROGRAM TEST'
C              WRITE(18,*)'PHASE= ',PHASER
C              WRITE(18,*)'PHASE SHIFT OPTION ENGAGED'
C              WRITE(18,*)'*****'
C              PHASER=PHASER*(PI/180.)

```

```

C      FIND MAXIMUM AND ZERO BELOW 1/10000 OF MAXIMUM.
C
C      AMAX=CABS(FOUT(2))
C
C      DO 902 I=3,SAMN/2
902    AMAX=AMAX1(AMAX,CABS(FOUT(I)))
C      CONTINUE
C
C      DO 336 I=2,SAMN/2
C      XXX=REAL(FOUT(I))
C      YYY=AIMAG(FOUT(I))
C      AMP=CABS(FOUT(I))
C      IF(AMP.LT.AMAX/10000.)GO TO 336
C      THETA=ATAN2(YYY,XXX)
C      THETA=PHASER+THETA
C      FOUT(I)=CMPLX(AMP*COS(THETA),AMP*SIN(THETA))
C      FOUT(SAMN-I+2)=CONJG(FOUT(I))
336    CONTINUE
C      ELSE
C      ENDIF
C
C      CALL FFT(SAMN,FOUT,+1.)
C
C      DO 777 I=1,SAMN
C      C(I)=REAL(FOUT(I))
777    CONTINUE
C
C      MAXIMUM DEFLECTION FOR SPEX WITH NO GAIN APPLIED IS
C      6000, SO THE MAXIMUM TRACE VALUE SHOULD BE SET TO
C      6000, AND ALL THE OTHER VALUES SHOULD BE SCALED
C      ACCORDINGLY.
C
C      FIND INDEX FOR DISPLAYING 512 MS OF DATA.
C
C      SAM=INT(SAMN/4.0)
C
C      XREALA(1)=ABS(C(1))
C
C      MXREAL=XREALA(1)
C      DO 998 MM=2,SAM-1
C      XREALA(MM)=ABS(C(MM))
C      MXREAL=AMAX1(MXREAL,XREALA(MM))
998    CONTINUE
C
C      NOW SCALE THE TRACE VALUES
C
C      SCALE=(6000./MXREAL)
C      DO 996 MM=1,SAM-1
C
C      *****
C      POLARITY
C      *****
C      C(MM)= C(MM)*SCALE
996    CONTINUE
C
C      FOR CONOCO DATA, ZERO OUT "EARLY REFLECTIONS" THAT WOULD
C      BE OBSCURED ON REAL STACKED DATA DUE TO MUTING.
C
C      DO 997 MM=1,180
C      C(MM)=0.0
997    CONTINUE
C
C
C

```



```

C*****
C SUBROUTINE ATTENU
C PURPOSE: TO CALCULATE AN ATTENUATION COEFFICIENT FOR EACH
C LAYER.
C INDEX OF VARIABLES:
C
C A * INDICATES THAT THE VARIABLE IS INPUT BY THE USER.
C THE MEANING OF * VARIABLES IS DISCUSSED NEAR THE BEGINNING
C OF THE PROGRAM.
C NUM=*
C
C OMEGA= AN ARRAY CONTAINING THE DISCREET FREQUENCY VALUES FOR
C WHICH THE RESPONSE IS CALCULATE. THE VALUE IN OMEGA(1)
C IS ZERO, FOR ZERO FREQUENCY, WHILE THAT IN OMEGA(4097)
C IS 2000 FOR A NYQUIST FREQUENCY OF 2000 HERTZ, SINCE
C .25 MS DATA IS BFING GENERATED.
C
C VEL5=*
C
C QUE=*
C
C ZU= A COEFFICIENT OF THE IMAGINARY COMPONENT OF VELOCITY. THIS
C IS THE TERM FACILITATING FREQUENCY DEPENDENT ATTENUATION
C MODELLING. ITS RELATIONSHIP TO VELOCITY AND 'Q' IS EVIDENT
C IN THE CODE.
C*****
C SUBROUTINE ATTENU(NUM,OMFGA,VEL5,QUE,ACDEF,ZU,QQP,INDI,ULAC)
C
C VARIABLE DECLARATIONS.
C
C INTEGER NUM,NUMB,QQP
C REAL OMEGA,VEL5(NUM+1),ZU(NUM+1),ACDEF(NUM+1),QUE(NUM+1)
C
C NUMB=NUM+1
C DO 5 I=1,NUMB
C IF(QQP,EQ,1)THEN
C ZU(I)=VEL5(I)/(2*QUE(I))
C ACDEF(I)=OMEGA*(ZU(I)/VEL5(I)**2)
C ELSE
C ACDEF(I)=0.0
C ENDIF
C CONTINUE
C
C IF 'INDI' EQUALS 1, THEN OMEGA IS A MAXIMUM CALCULATIONS
C ARE BEING PERFORMED FOR THE HIGHEST FREQUENCY, THIS
C CORRESPONDS TO MAXIMUM ATTENUATION FOR A GIVEN LAYER.
C
C IF(INDI,EQ,1)THEN
C DO 329 I=1,NUMB
C IF(QUE(I),LT,1.57)THEN
C WRITE(18,*)'*****'
C WRITE(18,*)'!!!!!!!!!!WARNING!!!!!!!!!!'
C WRITE(18,*)'Q IS TOO LOW FOR LAYER ',I
C WRITE(18,*)'*****'
C ELSE
C ENDIF

```

```

IF(ACOE(I),GT,ULAC)THEN
WRITE(18,*)'*****'
WRITE(18,*)'!!!!!!!!!!WARNING!!!!!!!!!!!!!!'
WRITE(18,*)'THE ATTENUATION COEFFICIENT FOR'
WRITE(18,*)'LAYER ',I,' IS HIGHER THAN THE MAXIMUM'
WRITE(18,*)'ATTENUATION COEFFICIENT SPECIFIED IN'
WRITE(18,*)'THE LIST OF INPUT PARAMETERS.'
WRITE(18,*)'*****'
ELSE
ENDIF
329 CONTINUE
ELSE
ENDIF
RETURN
END

C
C*****
C SUBROUTINE AIRAT
C PURPOSE: TO CALCULATE A RATIO OF COMPLEX ACOUSTIC IMPEDANCES
C ACROSS EACH ACTIVE INTERFACE.
C INDEX OF VARIABLES:
C
C VELS=*
C
C ZU= SEE SUBROUTINE ATTENU
C
C RHO=*
C
C NUM=*
C
C KAY= AN ARRAY CONTAINING THE RATIO OF COMPLEX ACOUSTIC
C IMPEDANCES. THERE IS ONE RATIO FOR EACH INTER-
C FACE. THE SURFACE IS NOT COUNTED AS AN INTERFACE.
C THIS IS TRUE THROUGHOUT THE PROGRAM.
C*****
C
C SUBROUTINE AIRAT(VELS,ZU,RHO,NUM,KAY)
C
C VARIABLE DECLARATIONS.
C
C REAL VELS(NUM+1),ZU(NUM+1),RHO(NUM+1)
C COMPLEX KAY(NUM),TOP,BOT
C
C DO 10 I=1,NUM
C TOP=CMPLX(VELS(I+1),ZU(I+1))
C BOT=CMPLX(VELS(I),ZU(I))
C KAY(I)=(TOP/BOT)*RHO(I+1)/RHO(I)
10 CONTINUE
RETURN
END

C
C*****
C SUBROUTINE CREFCO
C PURPOSE : TO CALCULATE A COMPLEX REFLECTION
C COEFFICIENT FOR EACH INTERFACE.
C INDEX OF VARIABLES:
C
C NUM=*
C
C KAY=SEE SUBROUTINE AIRAT,
C
C REFCO=AN ARRAY OF COMPLEX REFLECTION COEFFICIENTS,
C ONE FOR EACH INTERFACE.
C

```

```

C*****
C
C      SUBROUTINE CREFCO(NUM,KAY,REFCO)
C
C      VARIABLE DECLARATIONS
C
C      COMPLEX KAY(NUM),REFCO(NUM),NUMER,DENOM
C          DO 15 I=1,NUM
C              NUMER=1.0-KAY(I)
C              DENOM=1.0+KAY(I)
C              REFCO(I)=NUMER/DENOM
15      CONTINUE
C      RETURN
C      END
C
C*****
C      SUBROUTINE START
C
C      PURPOSE:          TO 'INITILIZE' THE UPWARD ITERATION
C                      BY APPLYING THE CONDITION THAT NO REFLECTION
C                      ARRIVES FROM BENEATH A GIVEN DPTH. THIS DEPTH
C                      IS THE BOTTOM ACTIVE INTERFACE OF THE MODEL.
C
C      INDEX OF VARIABLES:
C
C      REFCO= SEE SUBROUTINE CREFCO
C
C      X=*
C
C      VELS=*
C
C      OMEGA= SEE SUBROUTINE ATTENU.
C
C      NUM=*
C
C      SEED= THE CALCULATED RATIO OF UP TO DOWNGOING WAVE AMP-
C           LITUDES FOR THE POINT JUST BELOW THE NEXT-TO-
C           THE-BOTTOM INTERFACE. THIS IS THE VALUE USED
C           TO BEGIN THE ITERATION PROCESS IN SUBROUTINE
C           CARAT.
C*****
C      SUBROUTINE START(REFCO,X,ACDEF,VELS,OMEGA,NUM,SEED)
C
C      VARIABLE DECLARATIONS
C
C      COMPLEX REFCO(NUM),SEED,EXPON,TERMA
C      REAL X(NUM),ACDEF(NUM+1),VELS(NUM+1),ARG
C      REAL OMEGA,A,B,Y,TERMB
C
C      Y=2.718281828459045
C      ARG=(-2.)*(X(NUM)/VELS(NUM))*OMEGA
C      A=COS(ARG)
C      B=SIN(ARG)
C      TERMA=CMPLX(A,B)
C      EXPON=(-2.)*(ACDEF(NUM))*(X(NUM))
C      TERMB=Y**EXPON
C      SEED=REFCO(NUM)*TERMB*TERMA
C
C      RETURN
C      END
C

```

```

C*****
C      SUBROUTINE CARAT
C
C      PURPOSE:      TO ITERATE UPWARD THROUGH THE MODEL LAYERS
C                    UNTIL THE RATIO OF UP TO DOWN TRAVELLING WAVE AMP-
C                    LITUDES JUST BELOW THE SURFACE IS OBTAINED. THIS
C                    IS THE DEPENDENT VARIABLE "AMPRAT" USED IN CALCULAT-
C                    ING THE SEISMIC TRACE.
C
C      INDEX OF VARIABLES:
C
C      NUM=*
C
C      REFCO= SEE SUBROUTINE CREFCO.
C
C      ACOEF= SEE SUBROUTINE ATTENU.
C
C      X=*
C
C      VELS=*
C
C      OMEGA= SEE SUBROUTINE ATTENU.
C
C      SEED= SEE SUBROUTINE START.
C
C      LO= ZERO FREQUENCY.
C
C      HI= THE NYQUIST FREQUENCY TIMES 2 * PI.
C
C*****
C      SUBROUTINE CARAT(NUM,REFCO,ACOEF,X,VELS,OMEGA,SEED,LO,HI,
C      1  AMPRAT)
C      VARIABLE DECLARATIONS.
C
C      COMPLEX REFCO(NUM),AMPRAT,AMP,POWER,SEED
C      REAL    ACOEF(NUM+1),X(NUM),VELS(NUM+1)
C      REAL    OMEGA,A,B,Y,LO,HI
C
C      USE THE VALUE OF "SEED" ALREADY CALCULATED.
C
C      AMPRAT=SEED
C      Y=2.718281828459045
C      I=NUM-1
C      12  CONTINUE
C          A=ACOEF(I)*X(I)*2.0
C          A=-A
C          B=(X(I)/VELS(1))*OMEGA*2.0
C          B=-B
C          POWER=CMPLX(A,B)
C
C          AMP=(AMPRAT+REFCO(I))/(1+AMPRAT*REFCO(I))
C
C          AMPRAT=AMP*(Y**POWER)
C
C      IF(OMEGA.EQ.LO)THEN
C      WRITE(18,*)"*****"
C      WRITE(18,*)"THE VALUE OF AMPRAT FOR LAYER ",I
C      WRITE(18,*)"FOR ANGULAR FREQUENCY ",LO
C      WRITE(18,*)"*****"
C      WRITE(18,*)AMPRAT
C      ELSE
C      ENDIF
C
C

```

```

C
IF(OMEGA.EQ.HI)THEN
WRITE(18,*)"*****"
WRITE(18,*)"THE VALUE OF AMPRAT FOR LAYER ",I
WRITE(18,*)"FOR ANGULAR FREQUENCY ",HI
WRITE(18,*)"*****"
WRITE(18,*)AMPRAT
ELSE
ENDIF

C
C
I=I-1
IF(I.EQ.0)GO TO 20
GO TO 12
20 CONTINUE
RETURN
END

C
C*****
C SUBROUTINE FFT
C
C PURPOSE: TO CALCULATE AN INVERSE FOURIER TRANSFORM SO
C THAT THE FREQUENCY DOMAIN RESPONSE MAY BE DIS-
C PLAYED AS A TIME TRACE.
C
C INDEX OF VARIABLES.
C
C LX= THE LENGTH OF THE ARRAY FOR WHICH THE IFT IS
C CALCULATED.
C
C CX= THE TRACE VALUES, PASSED IN IN THE FREQUENCY DOMAIN
C AND PASSED OUT IN THE TIME DOMAIN.
C
C SIGNI= USE SIGNI= +1 FOR THE INVERSE FOURIER TRANSFORM.
C
C*****
C SUBROUTINE FFT(LX,CX,SIGNI)
C*****
C
C COMPLEX CX(LX),CARG,CEXP,CW,CTEMP
J=1
SC=SQRT(1./LX)
DO 30 I=1,LX
IF(I.GT.J)GO TO 10
CTEMP=CX(J)*SC
CX(J)=CX(I)*SC
CX(I)=CTEMP
10 M=LX/2
20 IF(J.LE.M)GO TO 30
J=J-M
M=M/2
IF(M.GE.1)GO TO 20
30 J=J+M
L=1
40 ISTEP=2*L
DO 50 M=1,L
CARG=(0.,1.)*(3.14159265*SIGNI*(M-1))/L
CW=CEXP(CARG)
DO 50 I=M,L,ISTEP
CTEMP=CW*CX(I+L)
CX(I+L)=CX(I)-CTEMP
50 CX(I)=CX(I)+CTEMP
L=ISTEP
IF(L.LT.LX)GO TO 40
RETURN
END

```

```

C*****
SUBROUTINE SPEX(HAMPLITUDE,NTRACE,NSAMPLE,INTERVAL)
C*****
C
C   VARIABLE DECLARATIONS
C
INTEGER*2 J,K,REEL1(1600),REEL2(200),TRHOUT(120)
DIMENSION HAMPLITUDE(NSAMPLE),HAA(700)
      REEL2(7)=NTRACE
      REEL2(9)=INTERVAL
      REEL2(10)=INTERVAL
      REEL2(11)=NSAMPLE
      REEL2(12)=NSAMPLE
      REEL2(13)=1
      REEL2(15)=1
      J=1600
      K=200
1  OPEN(2,MODE='BINARY',RFCFM='DYNAMIC',FILE=
   *':SI20:GGDAY:V.SYNSIZE',FORM='UNFORMATTED')
   WRITE(2) J,REEL1,K,REEL2
   J=120+(NSAMPLE*4)/2
   DO M=1,NTRACE
      TRHOUT(2)=M
      TRHOUT(4)=M
      TRHOUT(6)=1
      TRHOUT(8)=M
      TRHOUT(15)=1
      TRHOUT(58)=NSAMPLE
      TRHOUT(59)=INTERVAL
      IF(M.EQ,NTRACE) TRHOUT(88)=1
      TRHOUT(92)=1
      WRITE(2) J,TRHOUT,HAMPLITUDE
   END DO
   CLOSE(2)
   RETURN
END

```

Appendix 2 - Input parameters for Model Set 3, model 1.

) TY SYNIN	38.,14000.,2.3,120.
79	28.,10700.,2.2,100.
84.,5483.,2.0,20.	24.,14000.,2.3,120.
113.,7500.,2.1,30.	38.,10700.,2.2,100.
175.,11000.,2.2,138.	24.,14000.,2.3,120.
13.,16000.,2.4,50.	12.,10700.,2.2,100.
96.,13000.,2.2,144.	90.,14000.,2.3,120.
27.,14700.,2.3,200.	74.,10700.,2.2,100.
60.,13000.,2.2,144.	30.,14000.,2.3,120.
45.,14400.,2.3,160.	12.,10700.,2.2,100.
58.,13000.,2.2,144.	8.,14000.,2.3,120.
44.,14000.,2.3,160.	14.,10700.,2.2,100.
68.,12600.,2.2,144.	10.,14000.,2.3,120.
27.,14700.,2.3,200.	8.,10700.,2.2,100.
1.,14500.,2.29,50.	28.,14000.,2.3,120.
1.,14300.,2.27,50.	12.,10700.,2.2,100.
1.,14100.,2.25,50.	26.,14000.,2.3,120.
1.,13900.,2.23,50.	26.,10700.,2.2,100.
1.,13700.,2.21,50.	52.,14000.,2.3,120.
1.,13500.,2.19,50.	26.,10700.,2.2,100.
1.,13300.,2.17,50.	36.,14000.,2.3,120.
1.,13100.,2.15,50.	8.,10700.,2.2,100.
1.,12900.,2.13,50.	38.,14000.,2.3,120.
1.,12700.,2.11,50.	50.,10700.,2.2,100.
1.,12500.,2.09,50.	14.,16000.,2.35,200.
1.,12300.,2.07,50.	29.,10700.,2.2,100.
1.,12100.,2.05,50.	10.,14000.,2.3,120.
1.,11900.,2.03,50.	25.,10700.,2.2,100.
1.,11700.,2.03,50.	18.,14000.,2.3,120.
1.,11500.,2.03,50.	64.,12000.,2.2,100.
1.,11300.,2.03,50.	62.,15000.,2.3,200.
246.,15500.,1.9,50.	16.,12000.,2.2,130.
21.,10700.,2.2,100.	48.,15000.,2.3,200.
10.,16200.,2.3,150.	20.,12000.,2.2,130.
8.,10700.,2.2,100.	14.,15000.,2.3,180.
6.,16200.,2.3,150.	56.,12000.,2.2,130.
7.,10700.,2.2,100.	62.,15000.,2.3,180.
5.,16200.,2.3,150.	36.,12000.,2.2,130.
8.,10700.,2.2,100.	15000.,2.3,200.
8.,16200.,2.3,150.	.00025
21.,10700.,2.2,100.	1
8.,16200.,2.3,150.	2
42.,10700.,2.2,100.	90
	.5

Appendix 3 - Input parameters for Model Set 3, model 2.

) TY SYNIN	90.,14000.,2.3,120.
67	74.,10700.,2.2,100.
104.,5483.,2.0,20.	30.,14000.,2.3,120.
93.,7500.,2.1,30.	12.,10700.,2.2,100.
30.,8500.,2.2,138.	8.,14000.,2.3,120.
25.,8000.,2.2,150.	14.,10700.,2.2,100.
20.,7500.,2.2,150.	10.,14000.,2.3,120.
80.,9000.,2.2,138.	8.,10700.,2.2,100.
13.,14000.,2.4,50.	28.,14000.,2.3,120.
86.,12000.,2.2,144.	12.,10700.,2.2,100.
22.,13000.,2.3,200.	26.,14000.,2.3,120.
53.,12300.,2.2,144.	26.,10700.,2.2,100.
40.,13000.,2.3,160.	52.,14000.,2.3,120.
52.,12700.,2.2,144.	26.,10700.,2.2,100.
50.,13700.,2.3,160.	36.,14000.,2.3,120.
70.,13500.,2.2,144.	8.,10700.,2.2,100.
81.,14500.,2.2,150.	38.,14000.,2.3,120.
25.,13700.,2.2,50.	50.,10700.,2.2,100.
140.,16000.,2.1,50.	14.,16000.,2.35,200.
21.,10700.,2.2,100.	29.,10700.,2.2,100.
10.,16200.,2.3,150.	10.,14000.,2.3,120.
8.,10700.,2.2,100.	25.,10700.,2.2,100.
6.,16200.,2.3,150.	30.,14000.,2.3,120.
7.,10700.,2.2,100.	64.,12000.,2.2,100.
5.,16200.,2.3,150.	50.,15000.,2.3,200.
8.,10700.,2.2,100.	16.,12000.,2.2,130.
8.,16200.,2.3,150.	48.,15000.,2.3,200.
21.,10700.,2.2,100.	20.,12000.,2.2,130.
8.,16200.,2.3,150.	14.,15000.,2.3,190.
42.,10700.,2.2,100.	56.,12000.,2.2,130.
38.,14000.,2.3,120.	62.,15000.,2.3,180.
28.,12000.,2.2,100.	36.,12000.,2.2,130.
24.,14000.,2.3,120.	15000.,2.3,200.
38.,10700.,2.2,100.	.00025
24.,14000.,2.3,120.	1
12.,10700.,2.2,100.	2
	90
	.5